



What is the real cardiac anatomy?

Mori, Shumpei
Tretter, Justin T.
Spicer, Diane E.
Bolender, David L.
Anderson, Robert H.

(Citation)

Clinical Anatomy, 32(3):288-309

(Issue Date)

2019-04

(Resource Type)

journal article

(Version)

Version of Record

(Rights)

© 2019 The Authors. Clinical Anatomy published by Wiley Periodicals, Inc. on behalf of American Association of Clinical Anatomists.

This is an open access article under the terms of the Creative Commons Attribution - NonCommercial - NoDerivs License, which permits use and distribution in any medium,...



(URL)

<https://hdl.handle.net/20.500.14094/90005768>



REVIEW

What Is the Real Cardiac Anatomy?

SHUMPEI MORI ,^{1*} JUSTIN T. TRETTER,^{2,3} DIANE E. SPICER,⁴ DAVID L. BOLENDER,⁵
AND ROBERT H. ANDERSON ⁶

¹*Division of Cardiovascular Medicine, Department of Internal Medicine, Kobe University Graduate School of Medicine, Kobe, Japan*

²*Heart Institute, Cincinnati Children's Hospital Medical Center, Cincinnati, Ohio*

³*Department of Pediatrics, University of Cincinnati College of Medicine, Cincinnati, Ohio*

⁴*Department of Pediatric Cardiology, University of Florida, Gainesville, Florida*

⁵*Department of Cell Biology, Neurobiology and Anatomy, Medical College of Wisconsin, Milwaukee, Wisconsin*

⁶*Institute of Genetic Medicine, Newcastle University, Newcastle, United Kingdom*

The heart is a remarkably complex organ. Teaching its details to medical students and clinical trainees can be very difficult. Despite the complexity, accurate recognition of these details is a pre-requisite for the subsequent understanding of clinical cardiologists and cardiac surgeons. A recent publication promoted the benefits of virtual reconstructions in facilitating the initial understanding achieved by medical students. If such teaching is to achieve its greatest value, the datasets used to provide the virtual images should themselves be anatomically accurate. They should also take note of a basic rule of human anatomy, namely that components of all organs should be described as they are normally situated within the body. It is almost universal at present for textbooks of anatomy to illustrate the heart as if removed from the body and positioned on its apex, the so-called Valentine situation. In the years prior to the emergence of interventional techniques to treat cardiac diseases, this approach was of limited significance. Nowadays, therapeutic interventions are commonplace worldwide. Advances in three-dimensional imaging technology, furthermore, now mean that the separate components of the heart can readily be segmented, and then shown in attitudinally appropriate fashion. In this review, we demonstrate how such virtual dissection of computed tomographic datasets in attitudinally appropriate fashion reveals the true details of cardiac anatomy. The virtual approach to teaching the arrangement of the cardiac components has much to commend it. If it is to be used, nonetheless, the anatomical details on which the reconstructions are based must be accurate. Clin. Anat. 32:288–309, 2019. © 2019 The

Authors. *Clinical Anatomy* published by Wiley Periodicals, Inc. on behalf of American Association of Clinical Anatomists.

Key words: atrioventricular valves; coronary arteries; intracardiac anatomy; three-dimensional reconstruction; virtual dissection

INTRODUCTION

Cardiac anatomy is usually taught to medical students on the basis of examination of the cadaveric hearts opened and studied in the dissecting room. This approach, despite multiple limitations, has endured over the passage of time (Maresky et al., 2018). Such dissection of the heart, due to the

*Correspondence to: Shumpei Mori, Division of Cardiovascular Medicine, Department of Internal Medicine, Kobe University Graduate School of Medicine, 7-5-1 Kusunoki-cho, Chuo-ku, Kobe, Hyogo 650-0017, Japan. E-mail: shumpei_8@hotmail.com

Received 11 January 2019; Accepted 21 January 2019

Published online 13 February 2019 in Wiley Online Library (wileyonlinelibrary.com). DOI: 10.1002/ca.23340

© 2019 The Authors. *Clinical Anatomy* published by Wiley Periodicals, Inc. on behalf of American Association of Clinical Anatomists.

This is an open access article under the terms of the Creative Commons Attribution-NonCommercial-NoDerivs License, which permits use and distribution in any medium, provided the original work is properly cited, the use is non-commercial and no modifications or adaptations are made.

complex three-dimensional interrelations of its component parts, is known to be challenging (Stanford et al., 1994). It is also well recognized that the elements of anatomy taught in the first year of the medical curriculum do not always instill a lasting

knowledge (Hořda et al., 2019). Detailed knowledge of the structure and location of the cardiac components, nonetheless, is essential information for those diagnosing and treating cardiac disease. With the intention of improving the initial acquisition of this

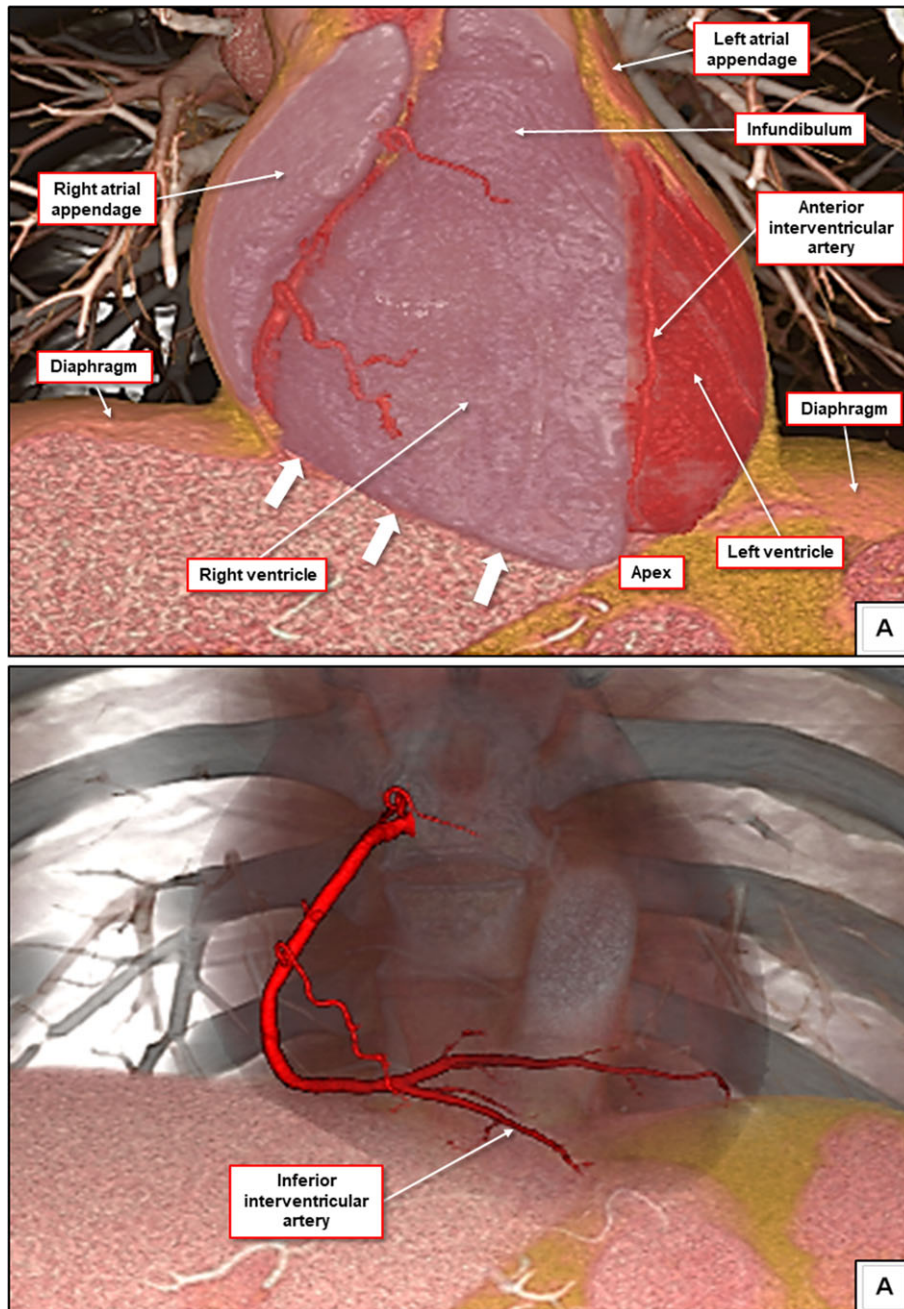


Fig. 1. The heart occupies the middle part of the mediastinum, but its long axis is markedly skewed relative to the long axis of body. Virtual dissection is able to show the heart in the so-called anatomical position. White arrows indicate the acute margin. Regarding the orientation cube attached in all following figures, the letters appeared as A, P, H, F, R, and L indicate anterior, posterior, superior (head), inferior (foot), right, and left, respectively. [Color figure can be viewed at wileyonlinelibrary.com]

knowledge, we have recently emphasized the value of virtual reconstructions of datasets obtained in the clinical setting (Mori et al., 2016a). When using a

similar approach, medical students were shown not only to enjoy the exposure to three-dimensional reconstructions, but also significantly to improve their

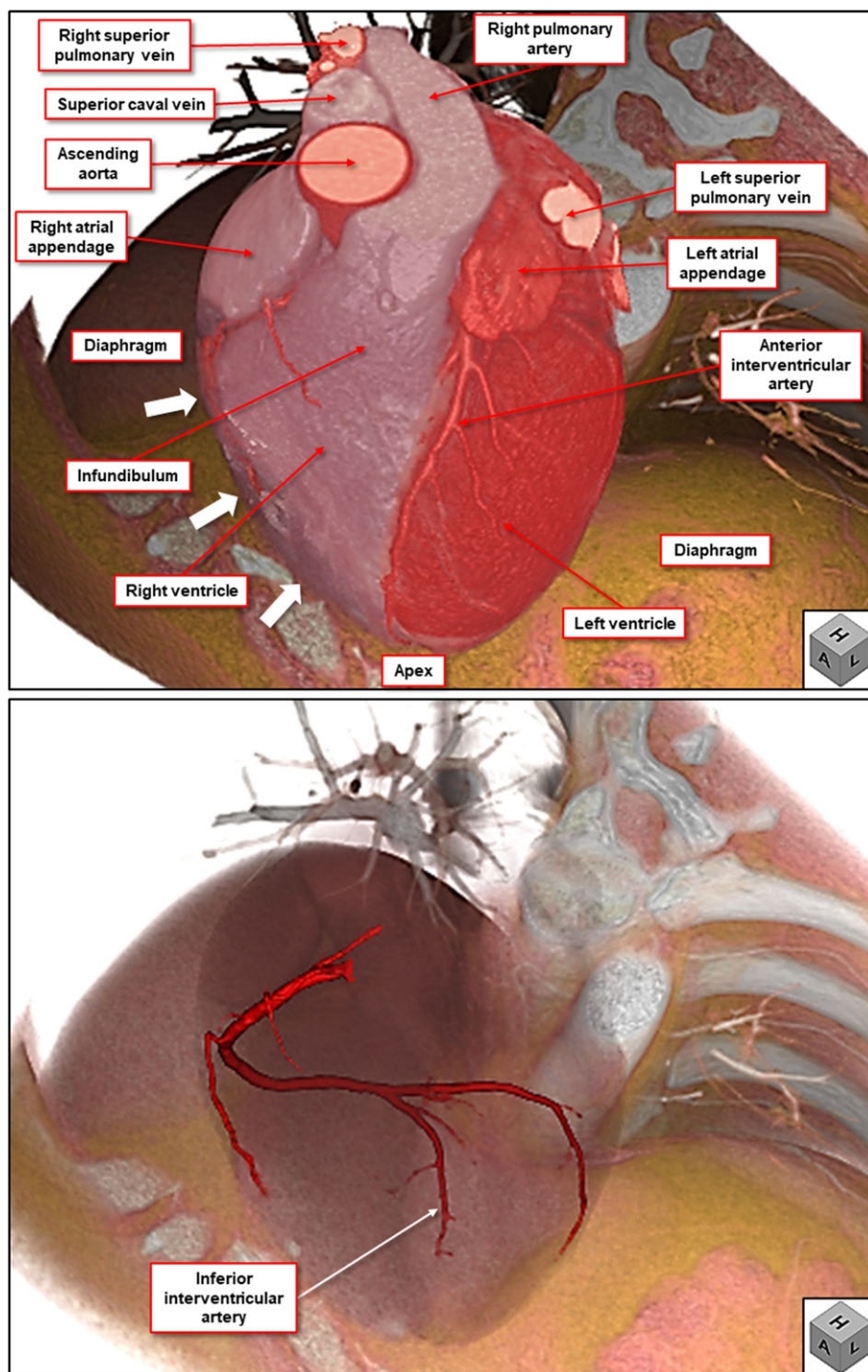


Fig. 2. A view of the heart from the left anterior oblique 45° and cranial 45° direction. Only in this projection, which is attitudinally inappropriate, can the heart be viewed in the so-called Valentine position. White arrows indicate the acute margin. [Color figure can be viewed at wileyonlinelibrary.com]

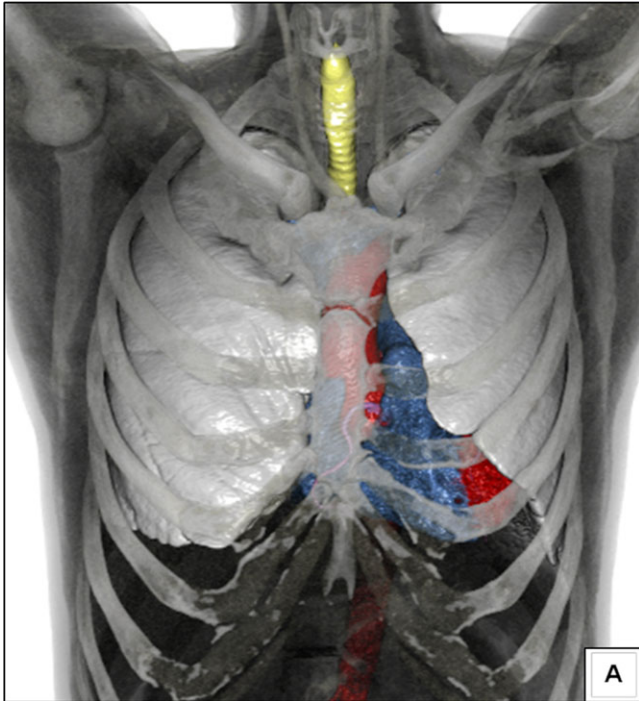


Fig. 3. This virtual dissection, revealing the thoracic contents, shows reason why echocardiographic windows are limited when using the transthoracic approach. [Color figure can be viewed at wileyonlinelibrary.com]

acquisition of the details of cardiac anatomy (Maresky et al., 2018). These developments in the technology of clinical imaging have made it possible to reveal all the details of cardiac anatomy without distorting the relationships to the intrathoracic structures (Mori et al., 2016a). There is no reason, therefore, why the nuances of cardiac anatomy should not now be taught to medical students using the attitudinally appropriate approach. This is more important for those who point to the advantages of virtual reality (Maresky et al., 2018; Anderson et al., 2018a). In this review, we show how such anatomically accurate virtual reconstruction is, indeed, capable of revealing the complex three-dimensional interrelations of its component parts.

IMAGE ACQUISITION AND RECONSTRUCTION

All images were reconstructed from full volume datasets obtained from adult patients. They had undergone electrocardiographically-gated contrast-enhanced cardiac computed tomography using commercially available multidetector-row scanners (SOMATOM Force, Siemens Healthcare, Forchheim, Germany). From the datasets available, we reconstructed selected examples showing normal features in the absence of any significant coronary arterial lesions or abnormal extracardiac findings, aside from the use of one dataset chosen from a patient with a pericardial effusion. Virtual dissections

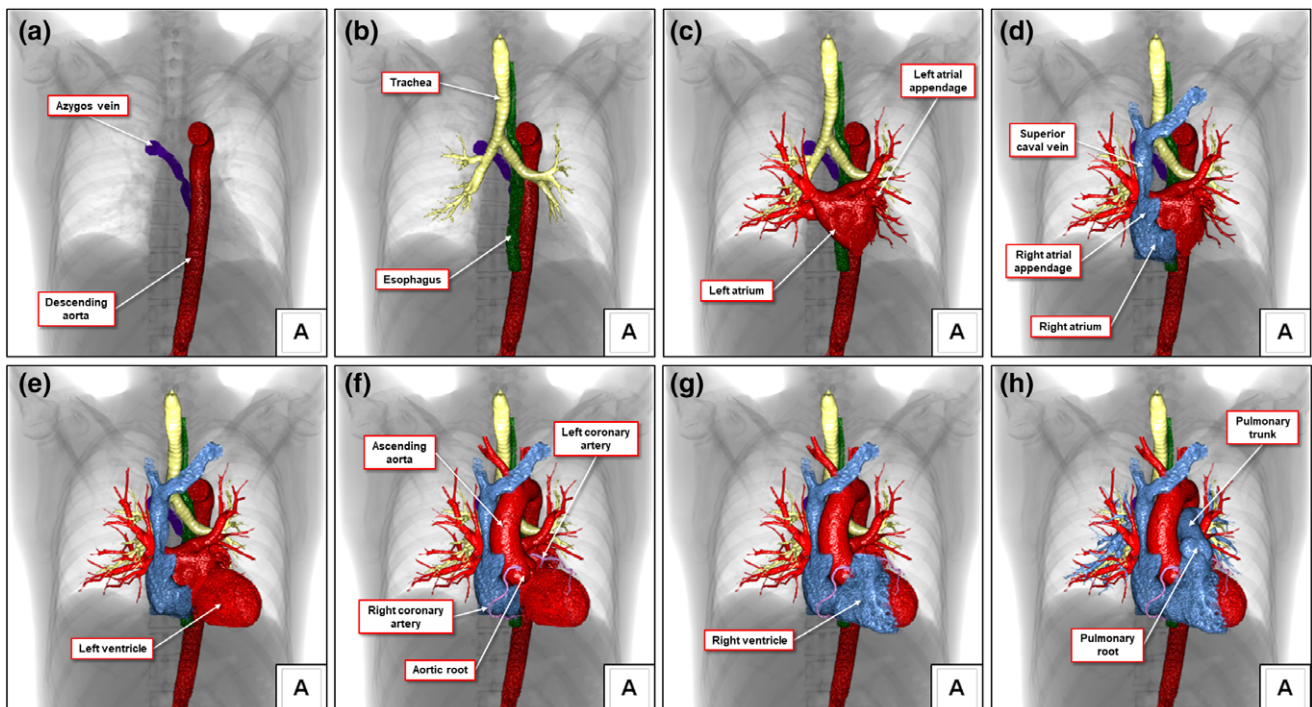


Fig. 4. The step-wise virtual dissection shows the contents of the middle mediastinum as viewed from the frontal direction. By tracking from the left upper (a) to the right lower panels (h), the components constructing and supporting the cardiac contour are demonstrated in order from the posterior direction. [Color figure can be viewed at wileyonlinelibrary.com]

and reconstructions were subsequently performed using a commercially available workstation (Ziostation2 ver. 2.4.2.3.; Ziosoft Inc., Tokyo, Japan).

PLACING THE HEART IN THE CHEST

One of the first rules of human anatomy is that all bodily parts should be described as viewed in the so-called anatomical position (Anderson and Loukas, 2009). This means that the heart should be described as it is normally positioned within the thorax (Fig. 1; Cosío et al., 1999; Anderson et al., 2013). It is difficult in the dissecting room, however, to assess the interrelationships of the cardiac components while the organ itself remains embedded within the mediastinum and encased by the thoracic skeleton and the lungs. It is almost certainly the need to remove the heart from the thorax so as to identify its individual components that has led to its usual description in so-called "Valentine" fashion. In this arrangement, which is currently followed in the greater majority of textbooks used for education of medical students, the organ is shown as positioned on its apex (Fig. 2). In the Valentine approach, the atrial chambers are shown inappropriately directly above the ventricles, with the right-sided structures shown as though truly right-sided relative to their allegedly left-sided counterparts (Anderson et al., 2013). When taking advantage of the images obtained from datasets prepared using the commercially available software used by clinicians, it is now possible to show the heart as it is properly situated within the thorax (Fig. 3).

SEGMENTING THE CARDIAC COMPONENTS

The great advantage of access to the clinical datasets as prepared using computed tomography is that it proves possible to segment not only the different components of the heart, but also the remaining thoracic organs. It is then possible to appropriately replace the significant parts of the heart within the body, and to reveal their attitudinally appropriate relationships (Anderson, 2015). The structures can be placed within the chest radiograph as viewed in frontal orientation, which is how the heart is viewed in the standard clinical examination (Fig. 4). Such virtual dissection shows that, within the middle component of the mediastinum, and directly behind the heart, the descending aorta is located within the left para-vertebral gutter, with the azygos vein crossing from left to right (Fig. 4a). The left atrium is the most posterior cardiac component, being located directly in front of the esophagus, with the asymmetric branching pattern of the trachea seen cranially (Fig. 4b,c). When the left ventricle is added to the reconstruction (Fig. 4e), it can be appreciated that its long axis of the ventricular mass is directed from right posterior to left anterior, with an additional inferior tilt (Fig. 5; Mori et al., 2017a). The axis does not run from up to down, as is suggested in the usual Valentine approach (Fig. 2). The addition of the ascending aorta provides

the crucial knowledge that its root springs from the centerpiece of the cardiac silhouette (Figs. 4f and 6; Dean et al., 1994; Anderson et al., 2000; Mori et al., 2017b). Completion of the cardiac silhouette with the addition of the so-called "right-sided" chambers shows that, although right-sided in part, they are also

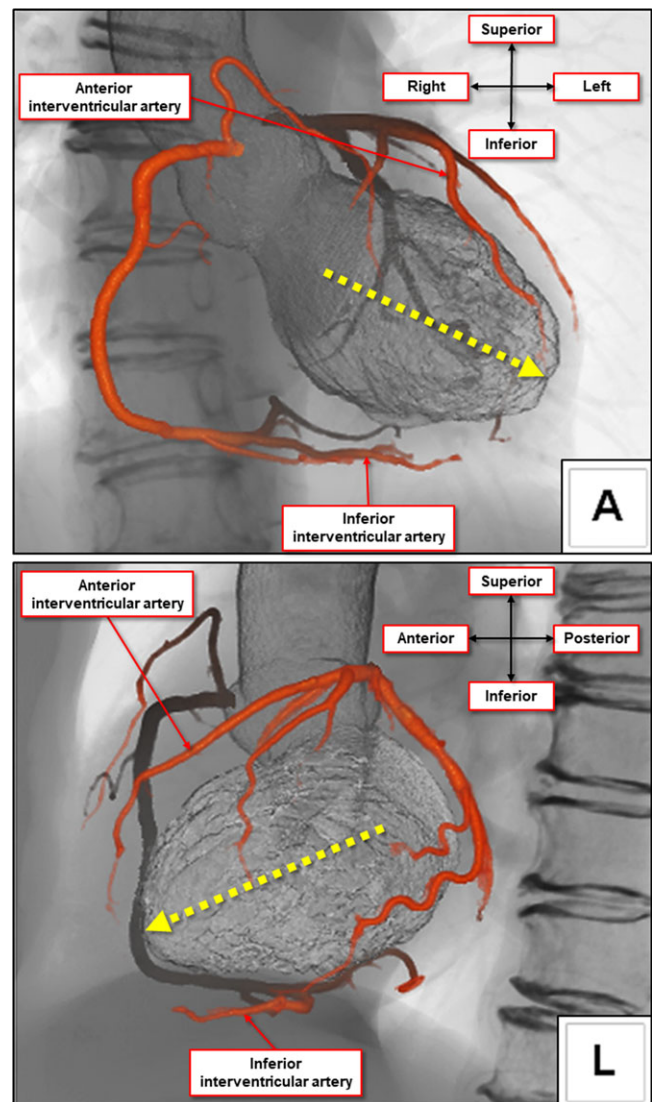


Fig. 5. The virtual images, shown in frontal (upper panel) and left lateral (lower panel) projections demonstrate how the branches of the coronary arteries delimit the extent of the left ventricle within the ventricular cone, with branches occupying the atrioventricular and interventricular grooves. The yellow dotted arrows show the long axis of the left ventricle, which runs leftward and inferiorly when traced from posterior to anterior. The images show how the artery occupying the inferior interventricular groove is never posterior to its counterpart in the anterior interventricular groove. It is a mistake to name this artery as being posterior and descending. [Color figure can be viewed at wileyonlinelibrary.com]

anteriorly positioned relative to their left-sided partners (Fig. 4d,g,h). In particular, the reconstruction now shows that the pulmonary root is anterior and leftward relative to the aortic root (Anderson et al., 2004). The intrapericardial component of the aorta can then be seen to ascend through the middle of the cardiac shadow,

but with marked spiraling relative to the pulmonary trunk, which extends caudally prior to bifurcating into the right and left pulmonary arteries (Fig. 4h; Anderson et al., 2003a, Anderson et al., 2016).

As with the left ventricle, the long axis of the right ventricle is similarly running from right posterior to

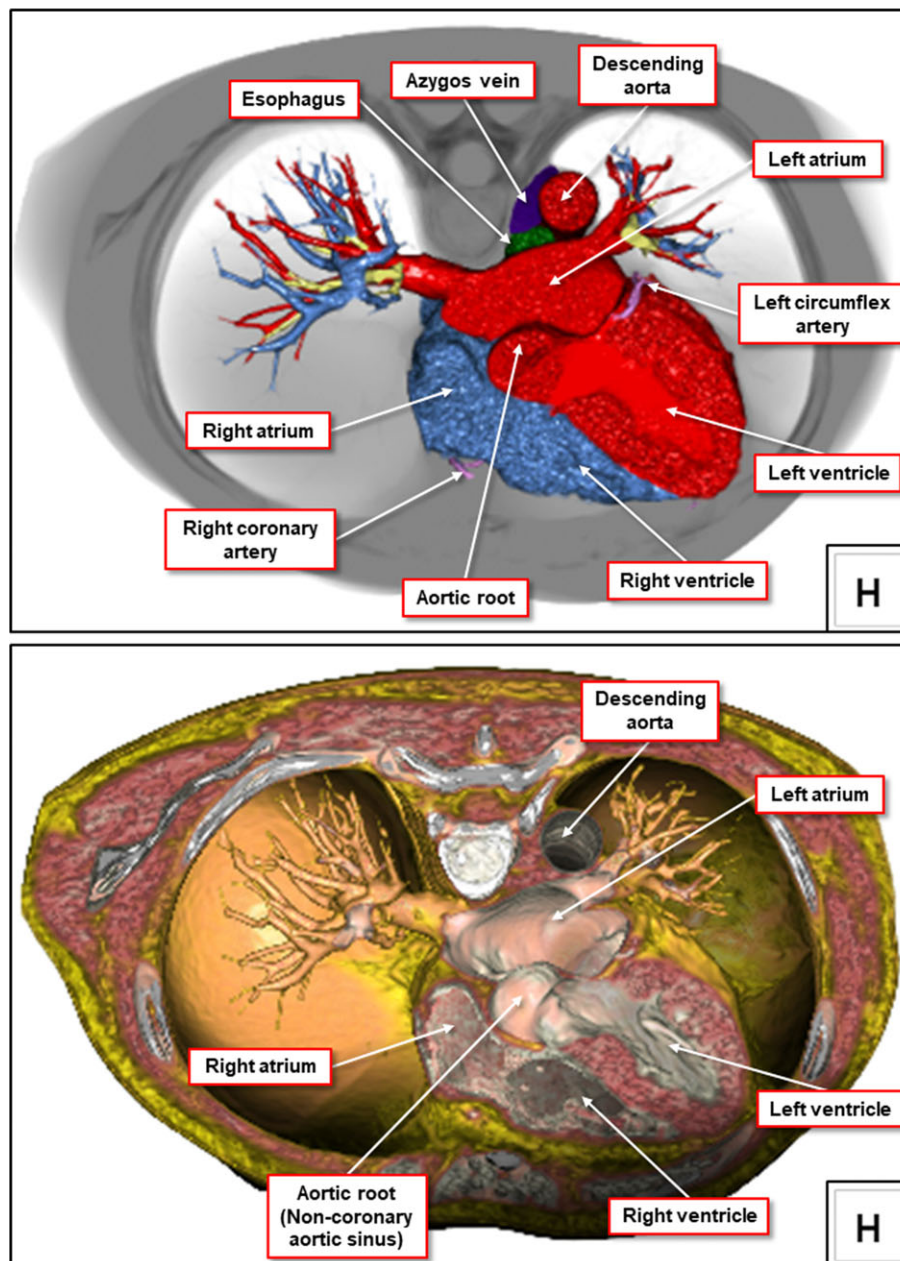


Fig. 6. When the so-called “five-chamber view” is created at the level of both inferior pulmonary veins, and then viewed from the superior direction, the spatial relationships between the cardiac chambers, as well as the central wedging of the aortic root, can be recognized in attitudinally appropriate fashion. The upper panel shows an endocast image mainly focusing on the relationships among each cavity, with the cavities removed in the lower panel to focus on the walls and septums (virtual dissection image). [Color figure can be viewed at wileyonlinelibrary.com]

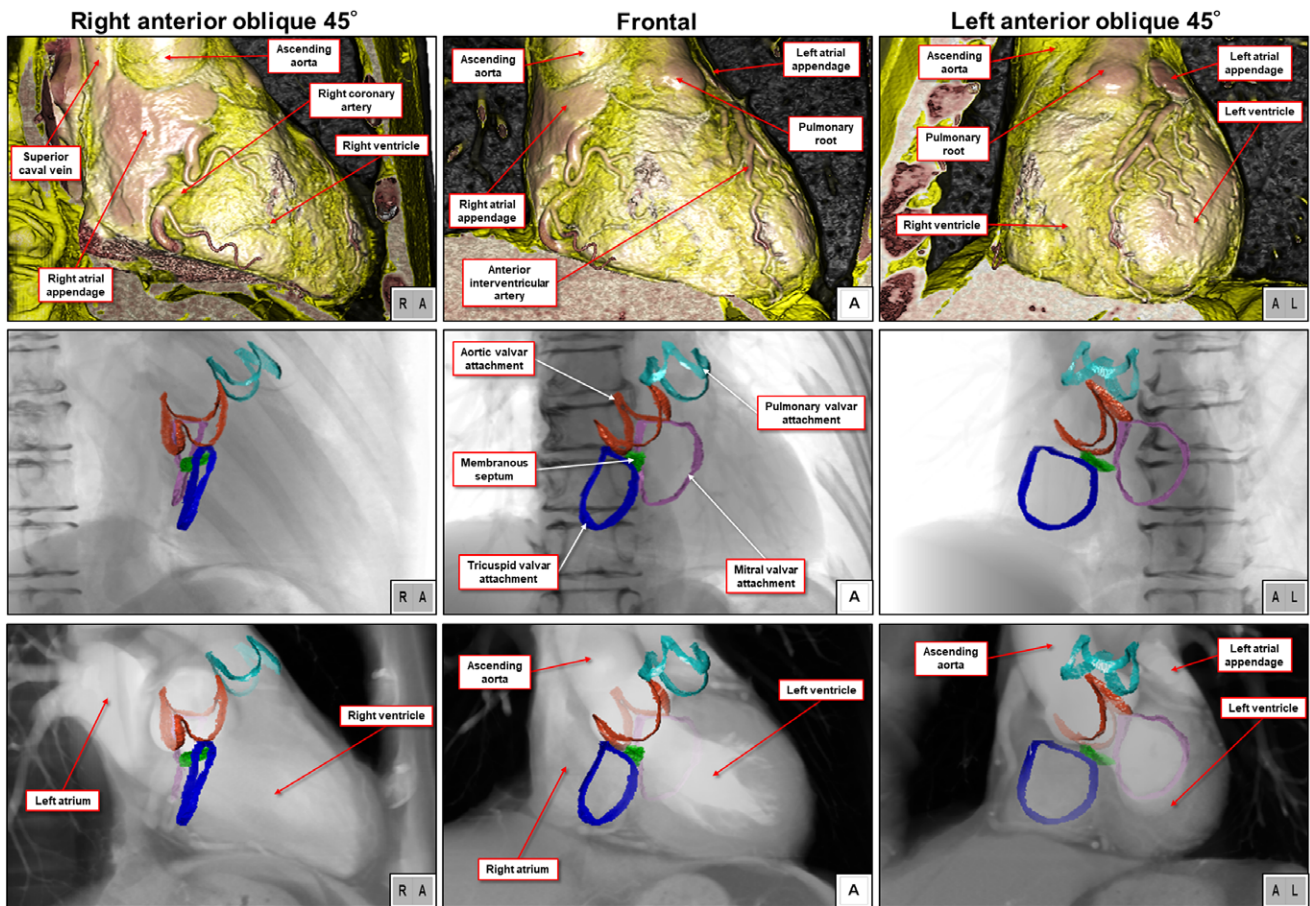


Fig. 7. The upper panels show the external aspect of the heart as viewed from the front (middle panel) and in right and left oblique projections (left-hand and right-hand panels). The middle row panels show the locations of the hinges of the valvar leaflets reconstructed within the cardiac contour, along with the membranous septum, as seen in the comparable projections. The lower panels show the hinges of the valvar leaflets incorporated in the multiplanar reconstruction sections, as seen in the comparable projections. The attachments of the aortic and pulmonary valves take the form of three-pronged coronets. [Color figure can be viewed at wileyonlinelibrary.com]

left anterior (Figs. 4h and 6; Mori et al., 2017a). Most significantly, by virtue of its position on the diaphragm, its parietal border, also known as the acute margin, is located inferiorly, rather than rightward as is suggested when the heart is viewed in Valentine orientation (Compare Figs. 1 and 2).

These true relationships, as revealed by segmentation of the cardiac components, combined with the ability of the virtual dissector to place them back within the cardiac silhouette (Fig. 4), show well why it is transesophageal echocardiographic interrogation that best reveals the details of the posteriorly positioned left atrium, as well as the descending aorta and, on occasion, the aortic arch (Willens and Kessler, 2000). It is only the tip of the appendage of the left atrium, located to the left side of the right ventricular infundibulum, which can be seen when the heart is viewed from the frontal direction (Fig. 1; Anderson

et al., 2004). Perhaps the most significant feature revealed by virtual dissection, however, is the central location of the aortic root within the base of the ventricular mass (Fig. 6; Anderson, 2000).

The inestimable added value of virtual dissection is that it also permits segmentation of the location of the hingelines of the valves which guard the junctions between the cardiac components, thus showing their relationships to each other (Anderson et al., 2004; Mori et al., 2016b). More importantly, it reveals their specific positions within the base of the ventricular mass (Fig. 7). Once the hinges of the leaflets of the valves have been placed within the cardiac silhouette, they can be viewed not only in frontal projection, which demonstrates their attitudinally appropriate relationships, but also in right and left oblique projections. It is these latter projections that show the structures as typically viewed by clinical cardiologists (Fig. 7—right

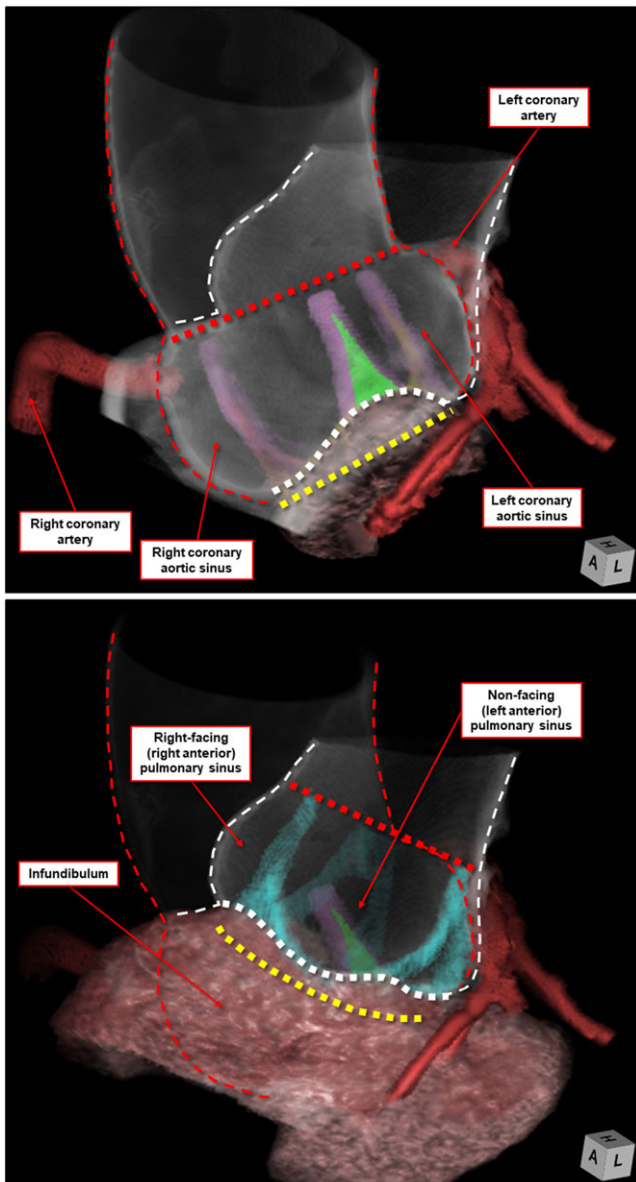


Fig. 8. The reconstructions show the aortic root (upper panel) and pulmonary root (lower panel) as viewed from the same direction. The red dotted lines indicate the sinutubular junction, while the white dotted lines denote the anatomical ventriculo-arterial junction. The yellow dotted lines indicate the plane of the virtual basal ring. [Color figure can be viewed at wileyonlinelibrary.com]

hand and left-hand panels). Having placed the valvar hinges within the silhouette, the most obvious feature is that, while the leaflets of the atrioventricular valves are hinged in relatively planar fashion, justifying the description of “annulus” for the atrioventricular valves, this is not the case for the arterial valves (Anderson et al., 2004; Mori et al., 2016b). When reconstructed in three-dimensions, the attachments

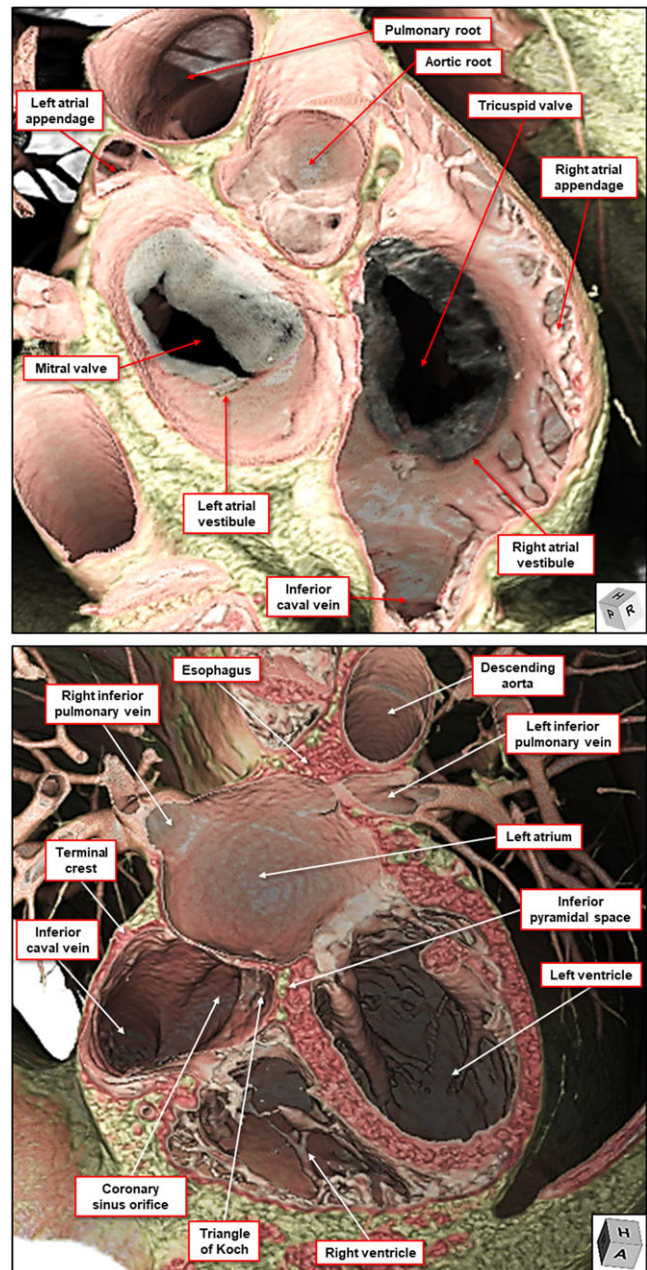


Fig. 9. The reconstruction in the upper panel shows that the pectinate muscles in the left atrium are confined within the tubular appendage, whereas in the right atrium, they encircle the vestibule of the tricuspid valve. When the so-called “four-chamber view” is created at the level of both inferior pulmonary veins, as shown in the lower panel, and then viewed from the superior direction, it is possible to appreciate the extent of the left atrial body. [Color figure can be viewed at wileyonlinelibrary.com]

of the arterial valvar leaflets take the form of three-pronged coronets (Fig. 7; Anderson, 2000; Anderson et al., 2004). The pulmonary root is located anteriorly

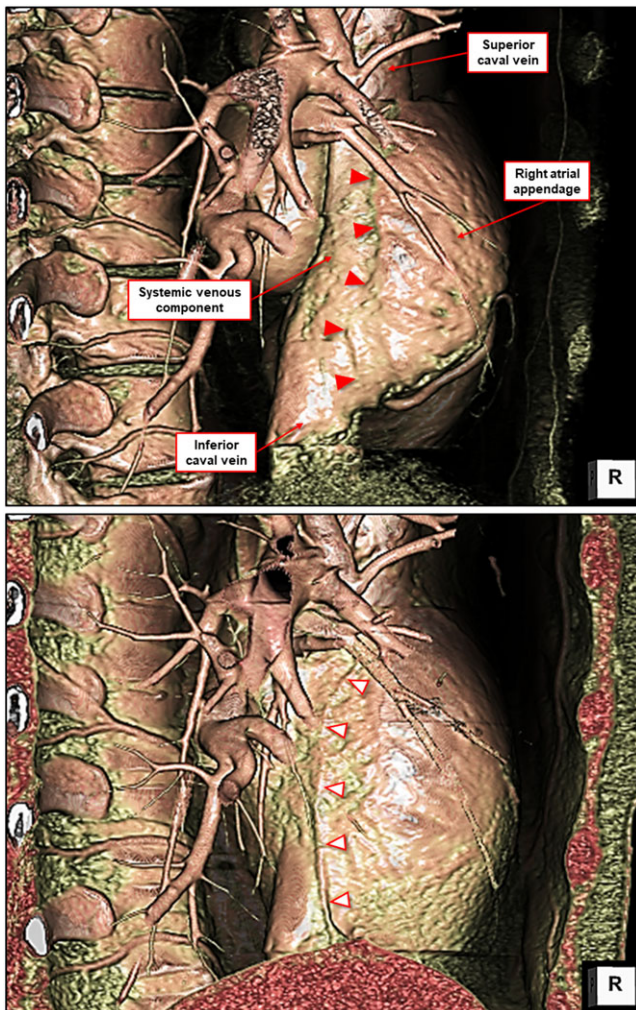


Fig. 10. The reconstruction in the upper panel shows the location of the terminal groove (red arrows), which forms the boundary between the venous component and appendage of the right atrium. When the adipose density is additionally reconstructed, as shown in the lower panel, it is possible also to demonstrate the course of phrenic nerve (red-rimmed white arrows). [Color figure can be viewed at wileyonlinelibrary.com]

and leftward relative to the aortic root (Fig. 7). Comparison of the three panels of Figure 7 also shows the marked discrepancy between the long axes of the two arterial roots. This reflects the spiraling of the outflow tract of the right ventricle as it swings from the inferiorly located apical component to the superiorly positioned pulmonary valve (Figs. 4 and 7; Anderson et al., 2003a, 2016). The reconstructions also show the problems that have arisen due to the different definitions provided for an “annulus” within the arterial roots (Sievers et al., 2012). The so-called “annulus” as defined by clinical echocardiographers is no more than a virtual plane, created by joining together the basal attachments of the semilunar

hinges (Tretter et al., 2016). It has no anatomical counterpart (Fig. 8).

ASSESSING THE ANATOMY OF THE CARDIAC COMPONENTS

Once having segmented the individual components of the heart, it is then an easy matter to assess each component separately, and to identify their individual parts. In this way, it can be shown that each atrial chamber possesses a body, a venous component, an appendage, and a vestibule (Anderson and Cook, 2007). The cavities themselves are separated by the atrial septum (Fig. 9). The atrial component of the developing heart tube forms the body of the developing chamber, which in the postnatal heart is almost exclusively committed to the left atrium (Anderson et al., 2003b; Jensen et al., 2017). The most consistent right atrial component is the appendage, making up the entirety of the anterior wall (Fig. 7). It is distinguished from the remainder of the atrium by its lining of pectinate muscles, which branch from the prominent terminal crest. This internal feature, corresponding to the external terminal groove, marks the border between the appendage and the venous component (Figs. 9–11). The systemic venous component of the atrium receives the superior caval vein at its roof, and the inferior caval vein in its floor (Figs. 10 and 11). Virtual dissection can also reveal the extent of the remnants of the valve of the systemic venous sinus, although not as accurately as true dissection. The remnants persist postnatally as the Eustachian and Thebesian valves. Examination of both true and virtual dissection shows that the so-called sub-Eustachian sinus of the right atrial vestibule is sub-Thebesian when the heart is assessed in an anatomically appropriate position (Fig. 12). The advantage of the virtual approach is that it becomes an easy matter to show the extent of the pectinate muscles which line the inner surface of the walls of the appendages. Such virtual dissection reveals that the pectinate muscles in the left atrium are confined within the tubular appendage. In the right atrium, in contrast, they encircle the vestibule of the tricuspid valve (Fig. 9). It is the morphology of the appendages that is now known to be the distinguishing criterion between the atrial chambers in the setting of congenital cardiac disease (Anderson, 2001). The ability to demonstrate the extent of the pectinate muscles, therefore, achieves particular clinical significance to correctly recognize cardiac isomerism (Uemura et al., 1995; Loomba et al., 2015; Mori et al., 2017c). Although it is also possible to open the hearts in the autopsy room while retaining their anatomically appropriate positions, the very act of opening them so as to reveal the internal features produces some degree of distortion. This is avoided when using virtual dissection, with the added advantage that the dissected chambers are seen in the form they take during their normal hemodynamic functioning. This virtual approach also reveals that the pulmonary venous component of the left atrium is positioned superiorly rather than posteriorly (Fig. 13). It also serves to emphasize

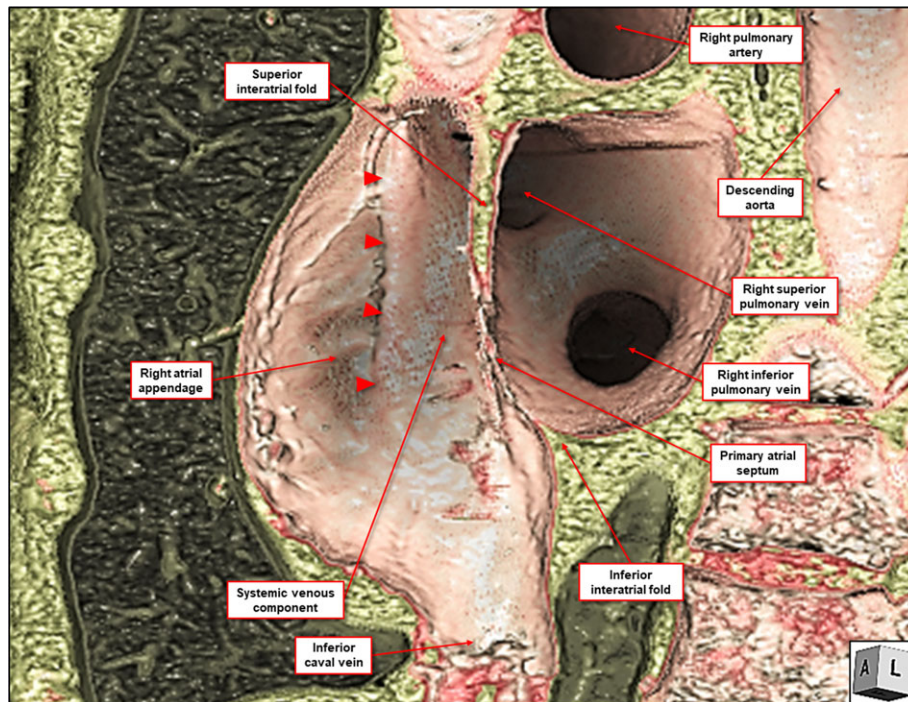


Fig. 11. Virtual dissection is then able to reveal the internal aspect of the right atrium showing the terminal crest (red arrows) interposed between the venous component and the appendage. Note the pectinate muscles branching at right angles from the terminal crest. [Color figure can be viewed at wileyonlinelibrary.com]

the extensive fold found between the tubular appendage and the termination of the left superior pulmonary vein (Fig. 14).

Virtual dissection also reveals the limited extent of the true atrial septum (Mori et al., 2016c; Mori et al., 2018a). The larger parts of the rims of the oval fossa are shown to be no more than folds between the right and left atrial walls. It is the floor of the fossa, derived from the primary atrial septum, along with the antero-inferior buttress, formed by muscularization of the vestibular spine and the mesenchymal cap carried on the leading edge of the primary septum (Jensen et al., 2017), which form the components that can be removed without transgressing on extracavitary space (Fig. 12). The antero-inferior buttress of the septum is itself contiguous with the septal component of the vestibule of the right atrium. It is in this area that there is off-setting of the hinges of the leaflets of the mitral and tricuspid valves (Spicer et al., 2014).

The coronary sinus, having traversed the left atrio-ventricular groove, opens into the vestibular area forming the floor of this space. It used to be thought that the area of overlap between the atrial wall of the space and the underlying ventricular myocardium formed an atrioventricular muscular septum (Becker and Anderson, 1982). Careful dissection of autopsied hearts showed this not to be the case, with the area between the atrial and ventricular walls being formed by a cranial extension of the fibroadipose tissue from

the inferior atrioventricular groove. The same details are shown by virtual dissection (Fig. 15). Such virtual dissection shows that the area is an open sandwich, rather than a true septum (Fig. 9; Dean et al., 1994; Anderson et al., 2000). The area in question is shown to be the inferior pyramidal space (Farré et al., 2010), with its superior extent limited by the atrioventricular component of the membranous septum (Figs. 12 and 15; Mori et al., 2015a). The inferior pyramidal space forms the floor of the triangle of Koch (Figs. 9, 12, 15, and 16; Mori et al., 2015b).

As is the case with the atrial chambers, both true and virtual dissections are able to demonstrate the extent of the ventricular myocardial cone (Mori et al., 2015c; Mori et al., 2016d). Using either technique, each ventricle within the cone can be shown to have inlet, apical trabecular, and outlet components (Fig. 16). The inlet components surround and support the atrio-ventricular valves, with their distal limits marked by the origins of the papillary muscles. The apical components have coarse trabeculations within the right ventricle, but fine cross-crossing trabeculations in the left ventricle (Fig. 16). It is the coarseness of the trabeculations that is the final arbiter of morphologically rightness or leftness when the heart is congenitally malformed (Anderson et al., 2004; Jacobs et al., 2007). These features are arguably better seen in cadaveric or autopsied hearts, although they can be distinguished subsequent to appropriate virtual dissection (Fig. 16). The structure

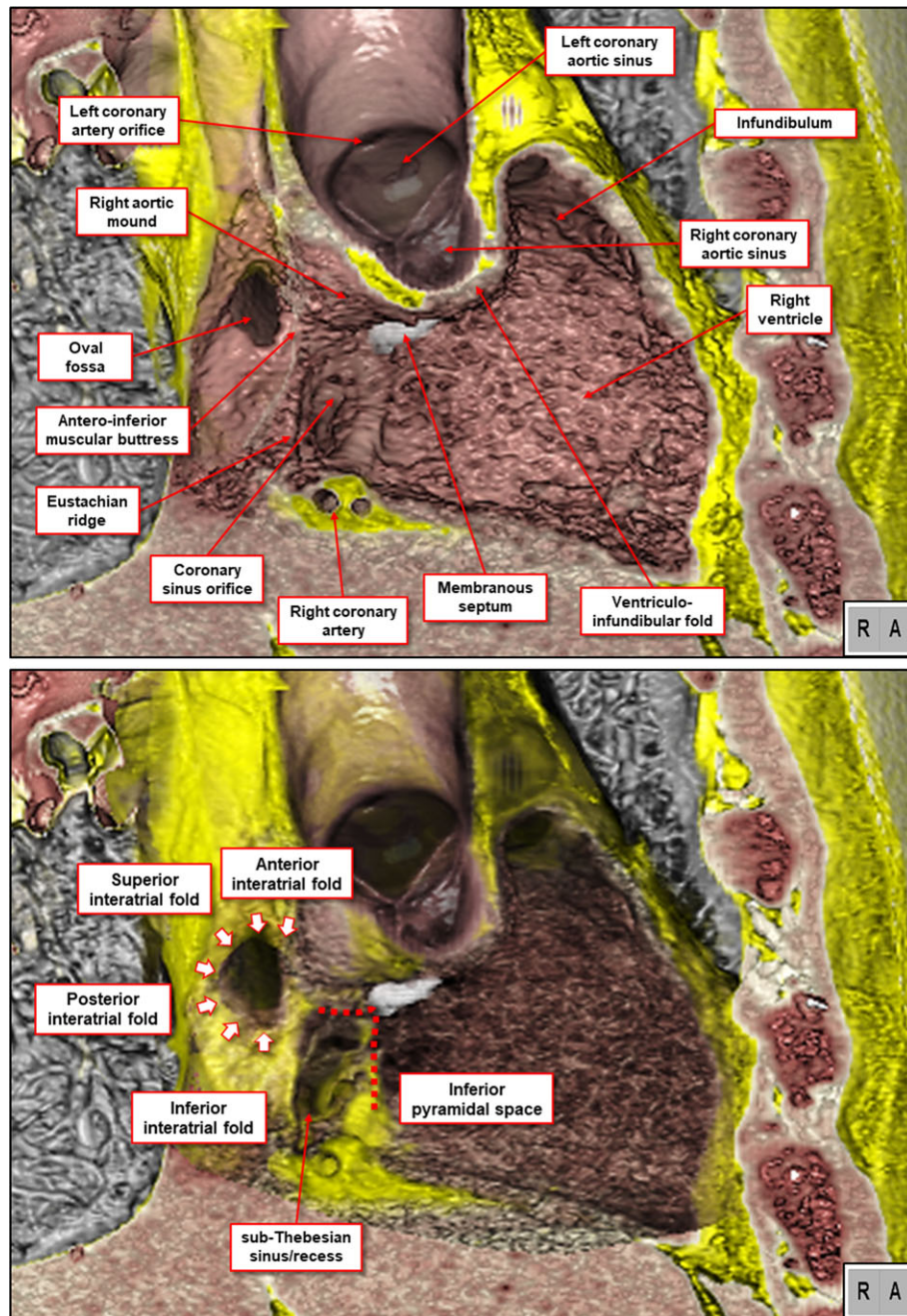


Fig. 12. The virtual dissections are viewed from the right anterior oblique 45° direction. The transparency of the surface myocardium is increased in the lower panel to demonstrate the interatrial folds. It also shows the location of the inferior pyramidal space at the septal aspect of the right atrium. The dissection also reveals that the so-called sub-Eustachian sinus is really sub-Thebesian. [Color figure can be viewed at wileyonlinelibrary.com]

of the outflow components also serves to provide another obvious morphological difference between the chambers when the heart itself is normally formed. The outlet is much abbreviated in the left ventricle, by virtue of the fibrous continuity between the leaflets of the

mitral and aortic valves (Fig. 16). The right ventricle, in contrast, possesses a long infundibulum, the distal part of which is a free-standing muscular sleeve. This lifts the leaflets of the pulmonary valve away from the base of the ventricular cone (Fig. 17; Lamers and Moorman,

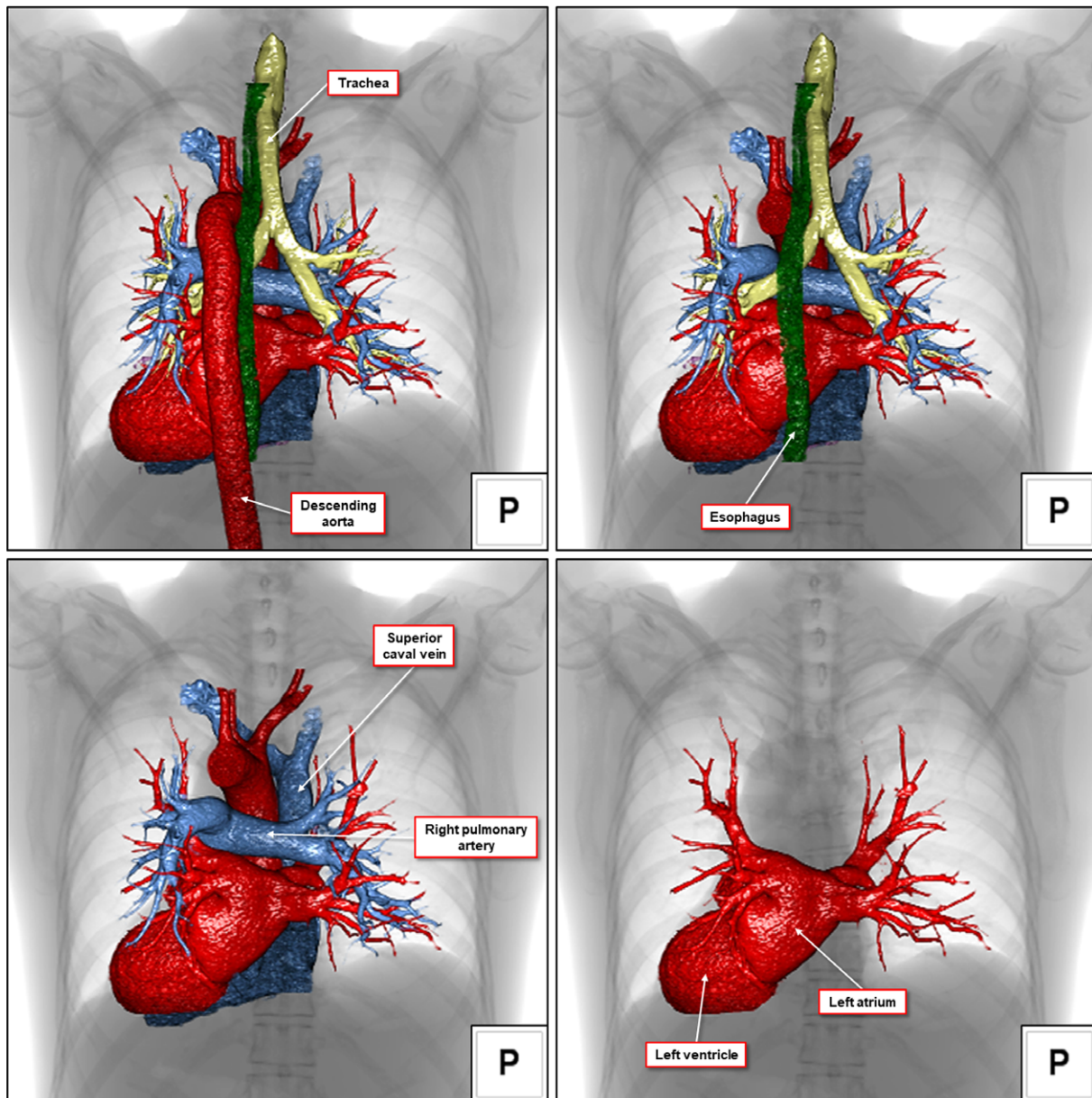


Fig. 13. The step-wise virtual dissection shows the cardiac components as viewed from the posterior direction. Moving from left to right, and from the upper to the lower panels, it was possible to remove the descending aorta (right upper panel), the esophagus and trachea (left lower panel), and the ascending aorta and right heart (right lower panel). [Color figure can be viewed at wileyonlinelibrary.com]

2002; Anderson et al., 2003a,b; Webb et al., 2003; Anderson et al., 2014). It is the presence of the free-standing infundibular sleeve that permits the entirety of the pulmonary root to be removed and used as an aortic autograft in the Ross procedure (Merrick et al., 2000). The inter-relationships of the valves in the two ventricles influence the septal morphology. Because of the deeply wedged location of the aortic root, the inferior part of the muscular ventricular septum separates the inlet of the right ventricle from the outlet of the left

(Fig. 18). And, because of the presence of the extensive free-standing infundibular sleeve, there is no muscular septum between the two outlets (Crucean et al., 2014). Thus, the ventricular septum is almost totally composed of the apical muscular septum. In the inner curvature of the heart, however, directly inferior to the aortic root, there is a small part of the septum that is fibrous (Figs. 12 and 17). This is conventionally described as the membranous septum. In many instances, this fibrous part of the septum is crossed by the hinge of the

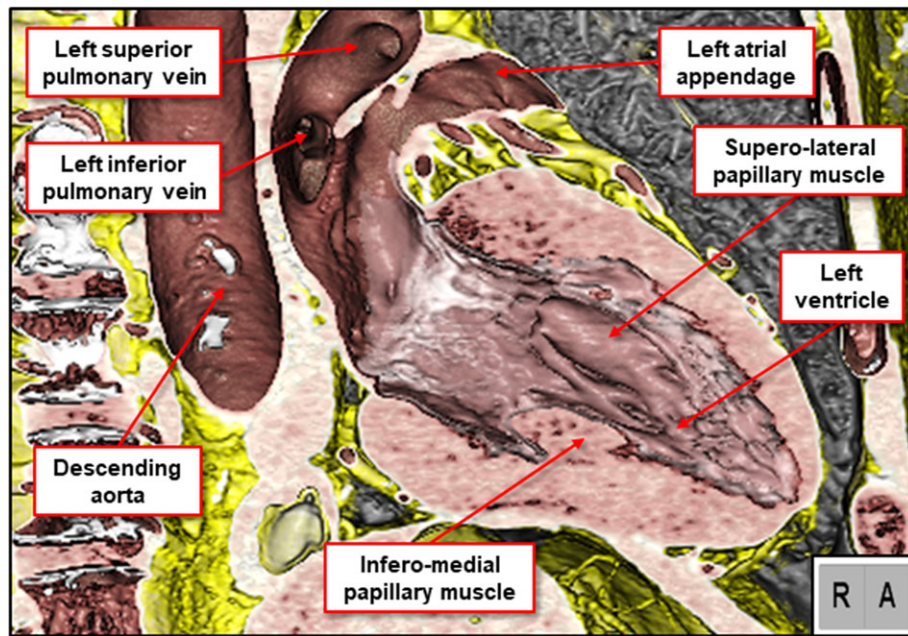


Fig. 14. The dissection reveals the so-called “two-chamber” image as seen from the right anterior oblique direction. It shows well the extensive fold which exists between the tubular left atrial appendage and the orifice of the left pulmonary veins. Note the relationship of the papillary muscles of the mitral valve. [Color figure can be viewed at wileyonlinelibrary.com]

septal leaflet of the tricuspid valve, dividing it into atrio-ventricular and interventricular components (Fig. 15; Anderson et al., 2004).

Virtual dissection shows particularly well the make-up of the third, or outlet, compartment of the heart. This is composed of the arterial roots, along with the intrapericardial components of the arterial trunks (Fig. 19; Anderson et al., 2016). The proximal border of each arterial root is the virtual basal ring formed by joining together the nadirs of the three semilunar leaflets of the arterial valves (Fig. 8; Anderson, 2000; Anderson et al., 2004; Anderson et al., 2018b). As already discussed, this plane has no anatomic counterpart, but is described by echocardiographers as the valvar annulus (Mori et al., 2017d). The distal extent of the roots is the sinutubular junction, where the semilunar hinges meet together at their circumference (Fig. 8). The proximal boundary of each root is the virtual basal plane. This line itself is proximal to the anatomic junction between the myocardium of the ventricular cone and the fibro-elastic sinuses of the roots which support the greater part of the semilunar hinges of the valvar leaflets. This potential paradox is explained by the fact that the basal hinges of some of the leaflets extend proximally relative to the anatomic ventriculo-arterial junction (Fig. 8). By virtue of this arrangement, crescents of myocardium are incorporated at the bases of each of the sinuses of the pulmonary root (Fig. 20; Anderson et al., 2018b, c). In the aortic root, however, because of the fibrous continuity found posteriorly between the leaflets of the

aortic and mitral valves, myocardium is incorporated into the bases of only the two valvar sinuses that give rise to the coronary arteries (Figs. 8 and 20; Mori et al., 2016a). The spaces on the ventricular aspect of the attachments of the valvar leaflets to the sinutubular junction are themselves filled by fibrous tissue, even though they are the distal parts of the ventricular chambers. These are the interleaflet triangles (Fig. 8; Sutton et al., 1995). The apical parts of these triangles separate the ventricular cavities from the pericardial space (Anderson, 2000; Mori et al., 2016d). The triangle between the non-coronary and right coronary sinuses of the aortic root is particularly significant (Tretter et al., 2018; Mori et al., 2018b), since it is continuous proximally with the membranous part of the septum (Fig. 15).

THE CORONARY VASCULATURE

The ability to segment the various cardiac components also extends to the branches of the coronary arteries and veins. The advantage of virtual dissection in this context is that it then shows these cardiac components as they are visualized by clinicians studying angiograms, and nowadays by using computed tomographic interrogation or magnetic resonance imaging. As already emphasized, when using virtual dissection, it proves possible not only to show the location of the various structures as seen relative to the frontal cardiac silhouette, but also in the oblique projections as used by clinicians to distinguish the

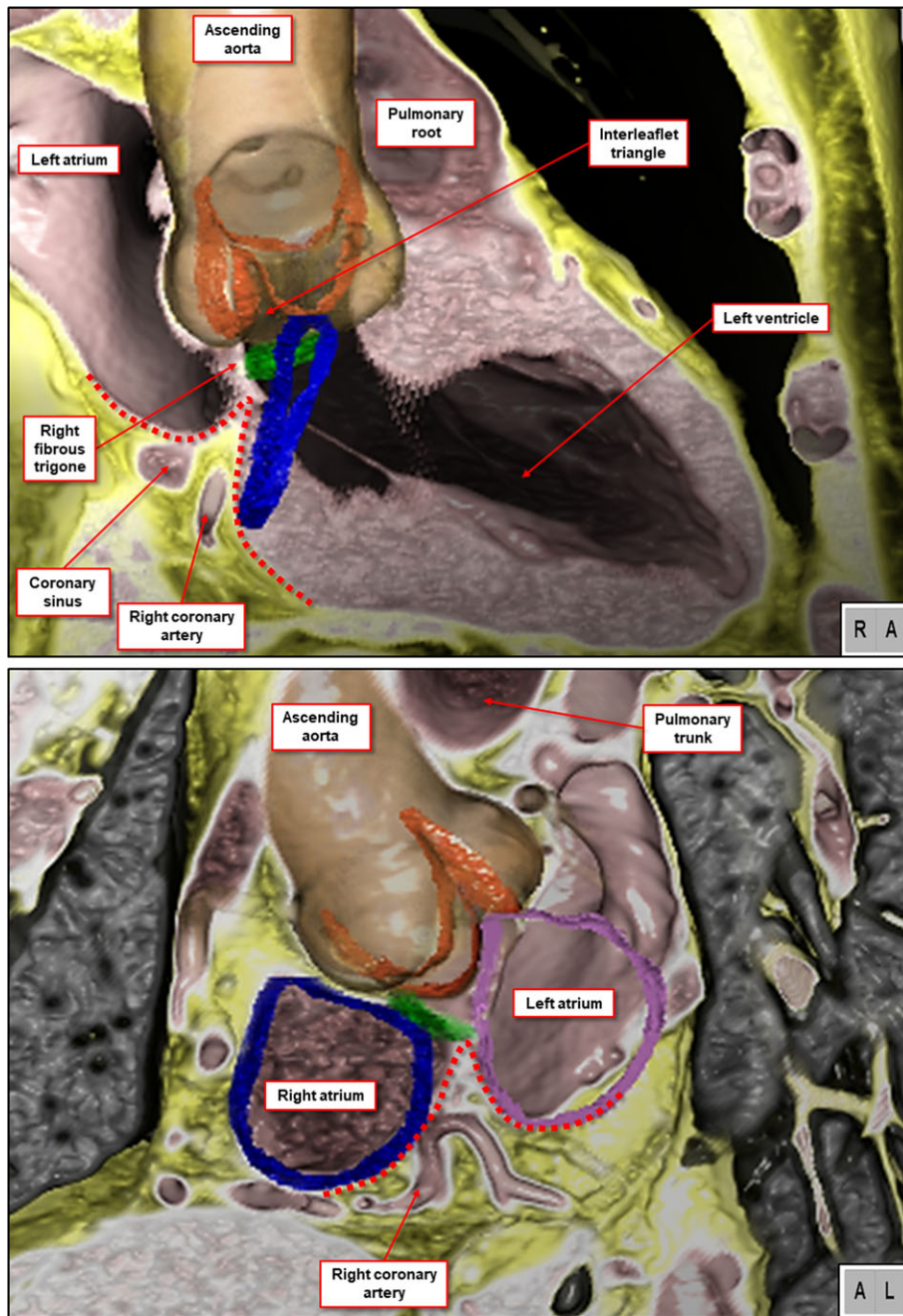


Fig. 15. The virtual dissections show that the inferior pyramidal space (red dotted lines) is filled by a cranial extension of the extracardiac fibro-adipose tissue that also occupies the atrioventricular junctions. The upper panel is a cut viewed in right anterior oblique projection, while the lower panel is seen from the left anterior oblique aspect, opening out the orifices of the atrioventricular valves. Pink and blue circles indicate the hinges of the mitral and tricuspid valvar leaflets, respectively. The green area denotes the membranous septum. See also Figure 7. [Color figure can be viewed at wileyonlinelibrary.com]

various vessels (Figs. 21 and 22). The images show how the coronary arteries are the initial branches of the aortic root, while the major venous tributaries

drain to the coronary sinus (Figs. 21 and 22). Although there are three aortic valvar sinuses, the coronary arteries take origin only from the two that are adjacent

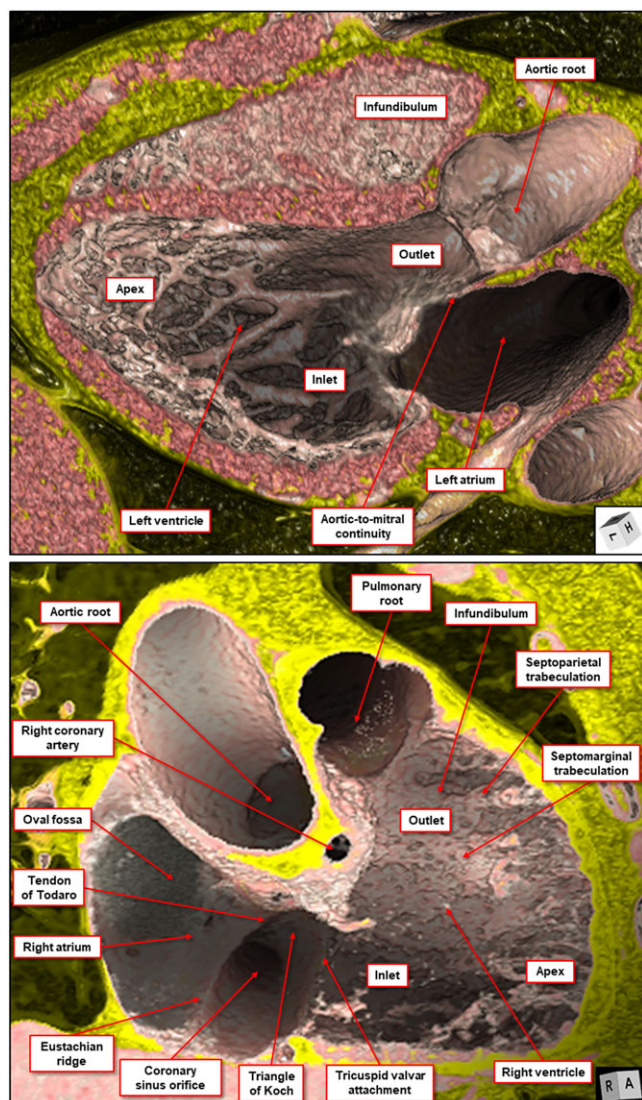


Fig. 16. The virtual dissections have been designed to show that left (upper panel) and right (lower panel) ventricle has inlet, apical trabecular, and outlet components. The triangle of Koch is the area bounded by the tendon of Todaro posteriorly, the central fibrous body (membranous septum and right fibrous trigone) apically, and the tricuspid valvar attachment anteriorly, with the orifice of the coronary sinus forming the inferior base (lower panel). [Color figure can be viewed at wileyonlinelibrary.com]

to the pulmonary root (Fig. 21). It is customary, nonetheless, to describe three major arteries. This is because the left coronary artery divides almost immediately into the anterior interventricular and circumflex arteries (Fig. 21). The circumflex and right coronary arteries then occupy the atrioventricular grooves, while the anterior interventricular artery, usually described as the left anterior descending artery, occupies the anterior

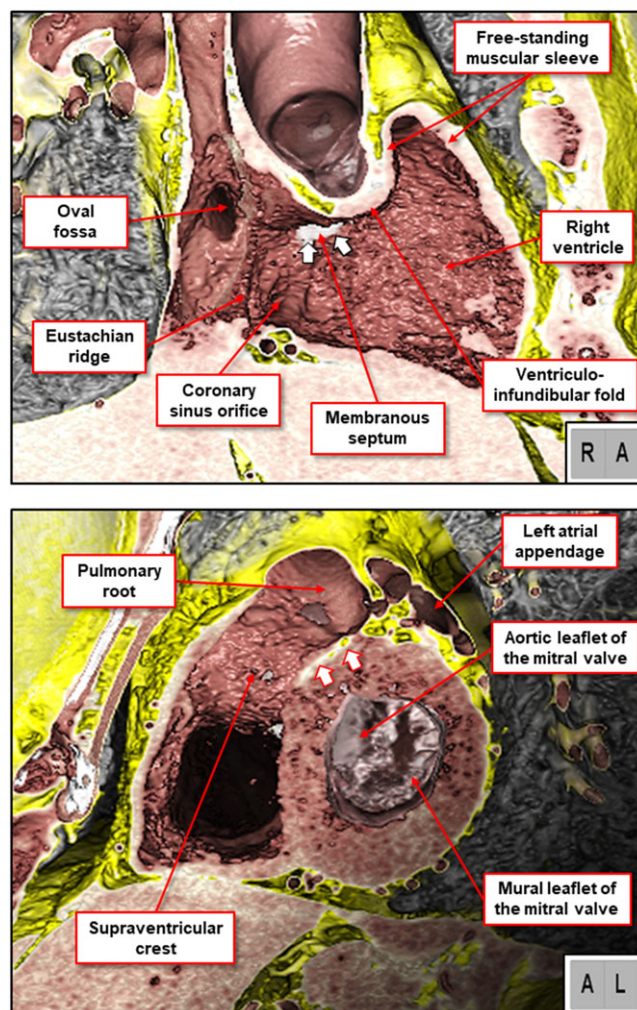


Fig. 17. The cuts of the heart show the arrangement as viewed from the right anterior and left anterior oblique projections in the upper and lower panels, respectively. The black-rimmed arrows in the upper panel indicate the crest of the muscular ventricular septum, which is the anticipated location of the atrioventricular conduction axis. The red rimmed arrows in the lower panel show the fibro-adipose tissue plane extending from the left ventricular free wall to the crest of the muscular ventricular septum, thus creating the free-standing pulmonary infundibulum. [Color figure can be viewed at wileyonlinelibrary.com]

interventricular groove (Figs. 1 and 2). Another prominent artery then occupies the interventricular groove found on the diaphragmatic aspect of the ventricular mass. This groove, and the coronary artery it contains, is located inferiorly (Fig. 1). Only when the heart is spuriously described in Valentine fashion can the artery be considered to be posterior and descending (Fig. 2). In reality, it is inferior and interventricular (Anderson and Loukas, 2009). It is accompanied by a coronary vein that would, in similar fashion, best be described as the

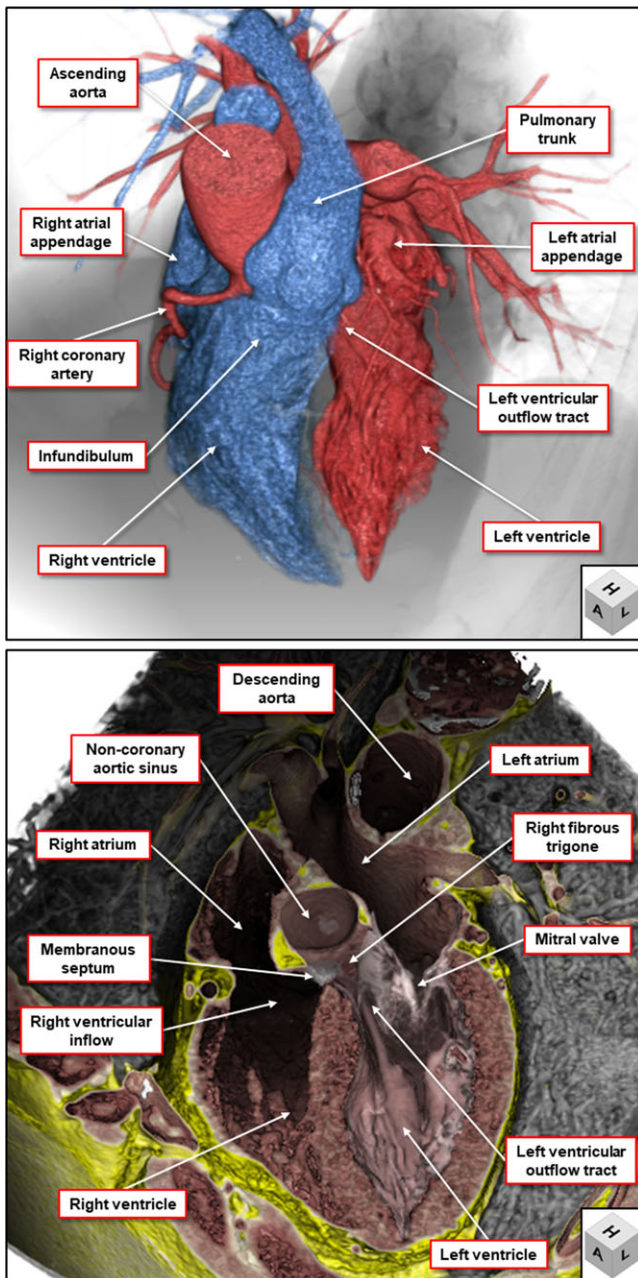


Fig. 18. The images show how it is views of the heart taken from the right anterior oblique direction that produce the Valentine position, along with rotation so as to place the apex downward. The upper panel is the endocast image, while the lower panel is the virtual dissection including the walls. [Color figure can be viewed at wileyonlinelibrary.com]

inferior interventricular vein (Fig. 22). The great cardiac vein accompanies the anterior interventricular and circumflex arteries. It is the union of this vein with the oblique vein of the left atrium, also known as the vein of Marshall, which marks the beginning of the coronary sinus.

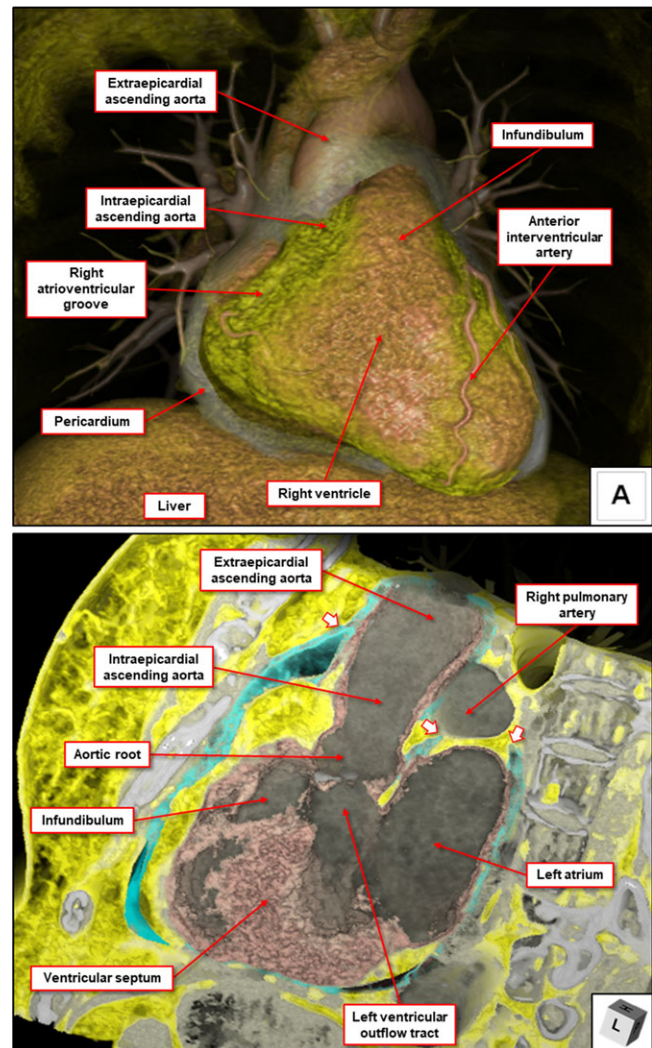


Fig. 19. The virtual dissections show how it is also possible to demonstrate the extent of the pericardial cavity, with the upper panel showing the heart as seen from the front. The arrows in the lower panel denote the pericardial reflections. These images were reconstructed from a patient with a pericardial effusion. [Color figure can be viewed at wileyonlinelibrary.com]

THE NEED FOR ATTITUDINALLY APPROPRIATE DESCRIPTION

The basic rules of human anatomy dictate that cranial, caudal, left, right, ventral, and dorsal directions should be referred to as superior, inferior, left, right, anterior, and posterior directions, respectively (Cosío et al., 1999; Anderson and Loukas, 2009; Anderson et al., 2013). This is the essence of description relative to the anatomical position. As we have already emphasized, it is this rule that should underscore the terms used to describe all bodily components. As with every other structure within the body, this attitudinally appropriate nomenclature should have traditionally been used

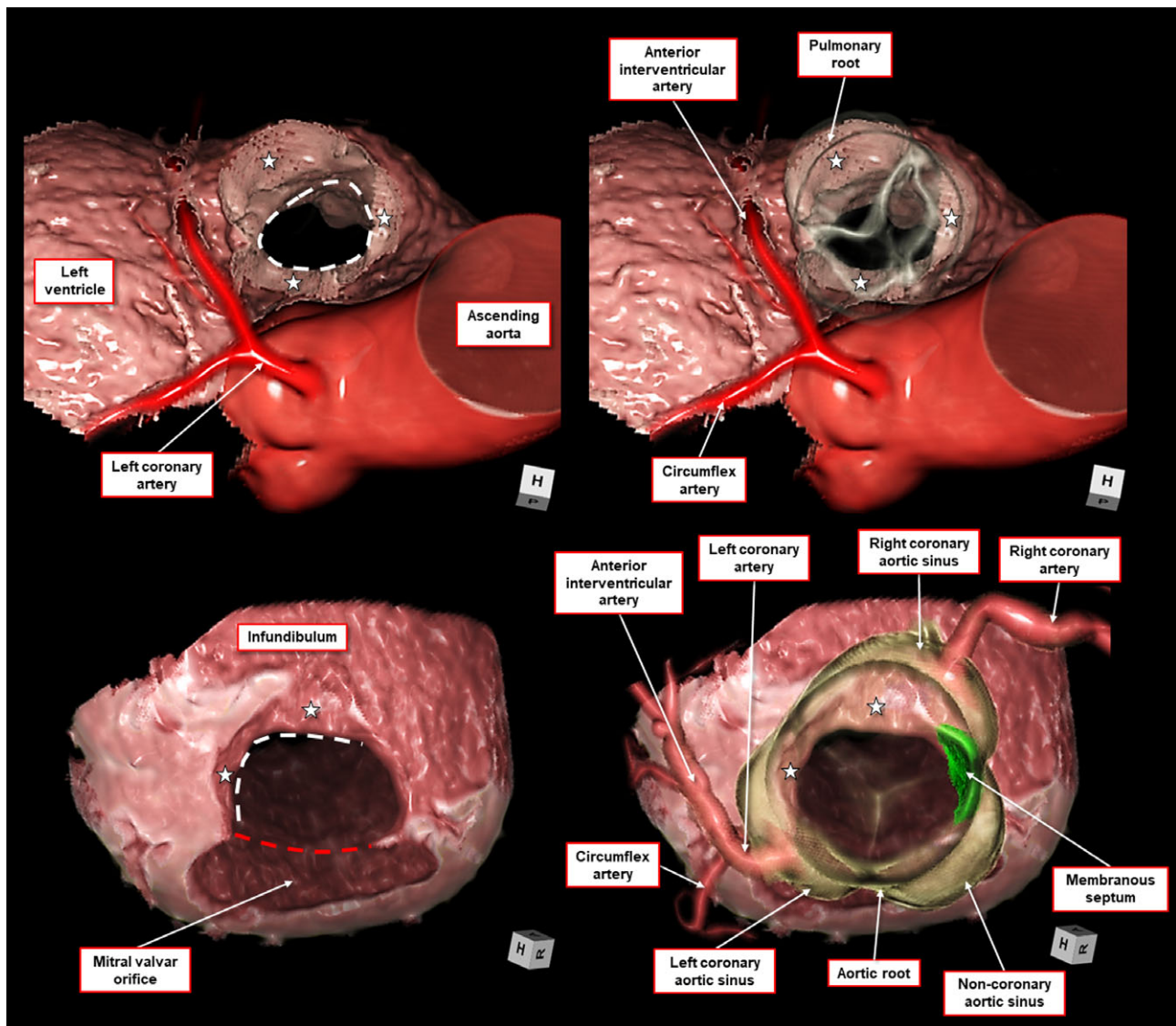


Fig. 20. The dissections are made to show the crescents of myocardium found at the bases of the arterial sinuses (white stars). The crescents are found at the base of each valvar sinus in the pulmonary root (upper panels), whereas they are found only at the bottom of the right coronary aortic sinus and anterior half of the left coronary aortic sinus in the aortic root (lower panels). The white dashed lines indicate the extent of muscular support on the virtual basal ring plane. The red dashed line denotes the aortic-to-mitral continuity. See also Figure 8. [Color figure can be viewed at wileyonlinelibrary.com]

to account for the detailed anatomy of cardiac structures. It is unfortunate that for centuries the heart has been described as if removed from the thorax and positioned on its apex, producing the so-called Valentine arrangement (Figs. 2 and 18). It is equally unfortunate that this inappropriate use of "Valentine" nomenclature remains the standard for current teaching of medical students, and continues to retain its currency by most of those practicing clinical cardiology. The increasing use of three-dimensional imaging techniques now serves

to emphasize the deficiencies of the non-attitudinal approach (Anderson, 2015). The deficiencies are now painfully obvious when images are viewed as prepared using the virtual dissection of computed tomographic datasets.

Perhaps the most egregious ongoing deficiency of the Valentine approach is the naming of the inferior interventricular artery. When imaging the heart in its correct anatomical location, the course of this artery is certainly not posterior, and it is barely descending.

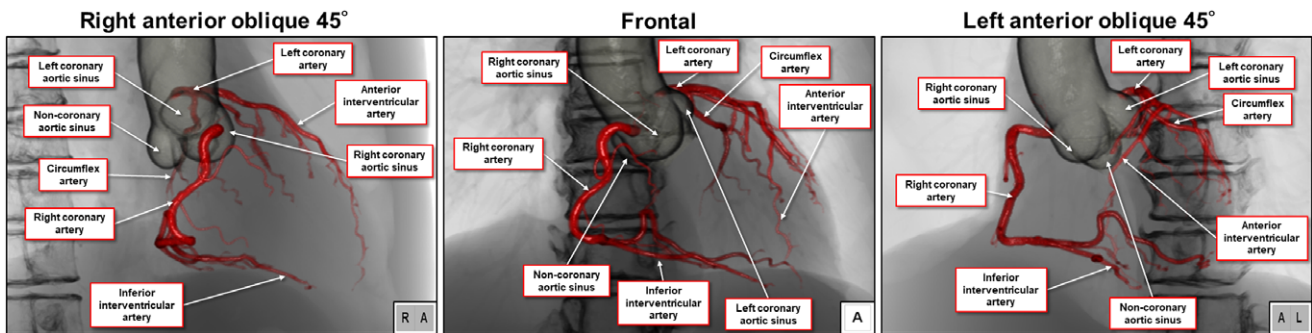


Fig. 21. The reconstructions show the coronary arteries as viewed from the frontal and right and left anterior oblique 45° directions. [Color figure can be viewed at wileyonlinelibrary.com]

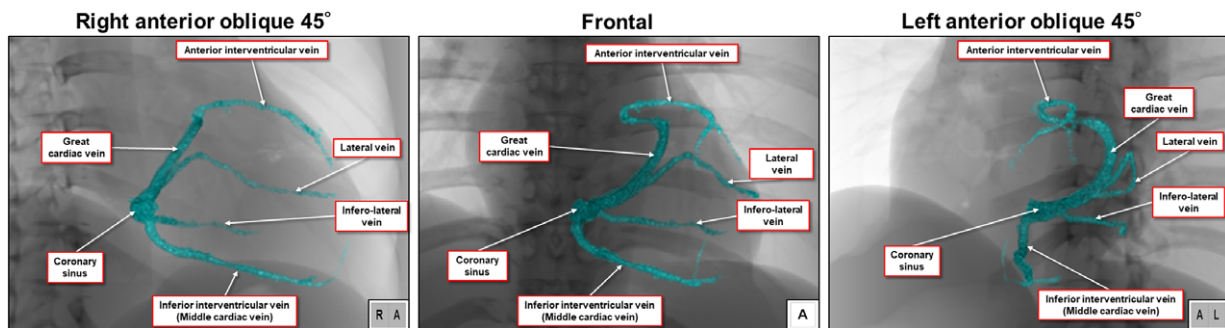


Fig. 22. Comparable reconstructions to those shown in Figure 21 show the coronary veins viewed from the frontal and right and left anterior oblique 45° directions. [Color figure can be viewed at wileyonlinelibrary.com]

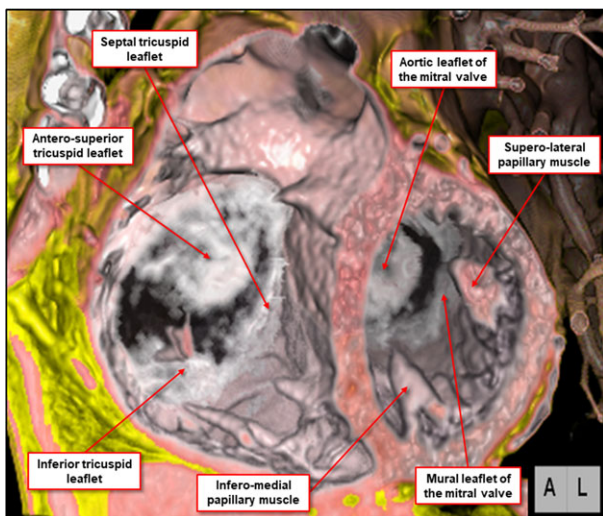


Fig. 23. The dissection made to show a short axis cut across the ventricular cone viewed in an anatomically appropriate fashion from the left anterior oblique 45° direction shows that the papillary muscles of the mitral valve are located infero-medially and supero-laterally. The leaflets of the tricuspid valve are positioned antero-superiorly, inferiorly, and septally. [Color figure can be viewed at wileyonlinelibrary.com]

Instead, the vessel, along with its accompanying vein, runs more-or-less horizontally on the inferior, or diaphragmatic, surface of the ventricular cone (Fig. 1). It is this location that explains why blockage of the artery produces inferior, and not posterior, myocardial infarction (Anderson and Loukas, 2009). The logic underscoring knowledge of the electrocardiogram, furthermore, is based firmly on the fact that the recordings are made and analyzed with the subject occupying the anatomical position (Mori et al., 2016a). Renaming the vessel as the inferior interventricular artery will surely facilitate the understanding of its actual location for medical students (Figs. 1, 5, and 21), which will be more important for them as they proceed to their clinical training.

The medical students, when they become clinical trainees, unfortunately, will encounter further problems. It is only when the heart is described on the basis of the Valentine position that it becomes possible to understand the current names given to the papillary muscles of the mitral valve. When observing the valve itself as it is positioned within the thorax, its leaflets are best described as being aortic and mural, although “anterior” and “posterior” are approximately accurate (Figs. 17, 23, and 24). Assessment of the locations of the papillary muscles, in contrast, leaves no question but they are located infero-medially and

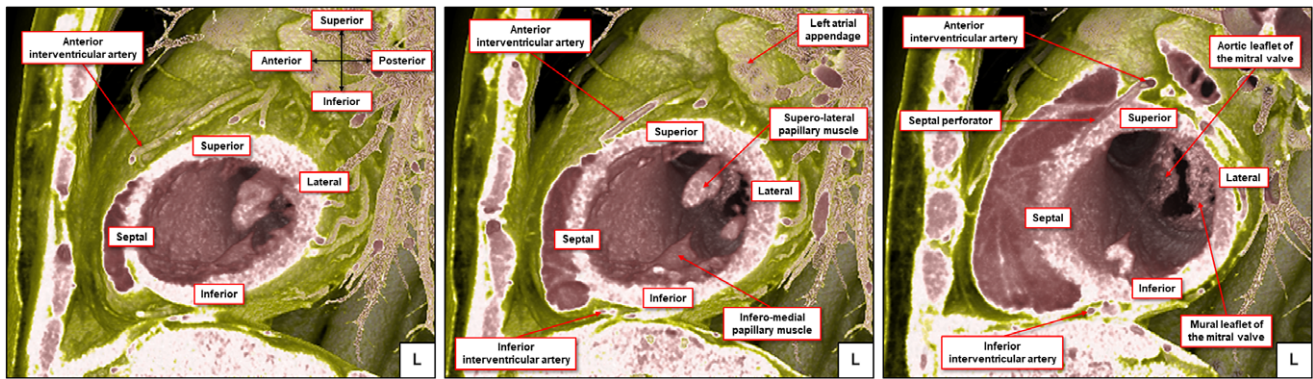


Fig. 24. As is demonstrated in the panels, which are sagittal cuts taken at apical (left hand), middle (middle panel), and basal (right hand) level of the anterior interventricular artery, the septal wall is always anterior to its lateral counterpart. It can also be seen that the anterior interventricular artery is always located superiorly relative to the inferior interventricular artery, and that it takes an antero-inferior course as it descends. It is also evident that describing the mitral leaflet as having anterior and posterior leaflets is not incorrect. The papillary muscles of the left ventricle, however, are not positioned “postero-septally” and antero-laterally”, as they are frequently described at the moment. It is also clear that the wall opposite the inferior quadrant of the ventricular cone is positioned superiorly, and not anteriorly. [Color figure can be viewed at wileyonlinelibrary.com]

supero-laterally (Figs. 14, 23, and 24). In similar fashion, it becomes obvious that the so-called “posterior” leaflet of the tricuspid valve is, in reality, the inferior leaflet (Anderson et al., 2013; Spicer et al., 2014; Mori et al., 2016b). It is the septal leaflet of the tricuspid valve that is located leftward and posteriorly within the right atrioventricular junction (Figs. 9 and 23).

INCONSISTENCIES IN THE SEGMENTATION OF THE LEFT VENTRICULAR CONE

Comparison of Figures 1 and 2 shows that the superior and inferior walls of the left ventricular cone, as seen in attitudinally appropriate orientation, are equivalent to those described as being anterior and posterior by those using the Valentine approach. The inappropriate use of “posterior” in this regard has been recognized when accounting for the inferior wall of the left ventricle by those using echocardiography (Cerqueira et al., 2002; Lang et al., 2015). It is difficult to understand, therefore, why those accepting the inappropriate use of “posterior” should continue to be use anterior rather than superior when describing the opposite wall (Lang et al., 2015). The antonym of “inferior” must surely be “superior”? The situation, however, is not as clear cut as it might seem. This is because the long axis of the left ventricle is not directly anterior relative to the spine and sternum, but rather is directed in left anterior and slightly inferior fashion (Figs. 5 and 6; Loukas et al., 2016; Mori et al., 2017a). Thus, when assessing short axis images of the ventricular cone in left anterior oblique projection, the side of the cone seen to the left hand is directed not only anteriorly but also rightward. The

component of the wall seen to the right hand is similarly located posteriorly and leftward, rather than being directly posterior, as we have suggested in our previous papers (Cosío et al., 1999; Anderson and Mori, 2016). When we then consider the walls of the ventricular cone themselves, nonetheless, it remains the case that, in any given sagittal cut through the ventricular cone, the septal wall is always anterior to its lateral counterpart (Fig. 24). If, in this context, we assess the course of the interventricular coronary artery universally described as being “anterior”, we find that the vessel, as it extends anteriorly and leftward from its aortic sinus origin, is consistently positioned superiorly relative to its partner occupying the inferior interventricular groove. The latter artery, as discussed, is located inferiorly rather than posteriorly. Its blockage produces inferior myocardial infarction. Blockage of the artery occupying the superior interventricular groove, nonetheless, does lead to antero-septal infarction. Proposals to rename this vessel as being the superior interventricular artery, with the consequence of correcting “antero-septal infarction” to “supero-septal infarction”, might be considered a step too far. But we cannot disguise the fact that the antonym of the inferior is superior. And, even though the long axis of the ventricular cone is tilted inferiorly and leftward when traced from posterior to anterior (Fig. 5), it is always the case that the septal wall is always anterior to its lateral counterpart in any given sagittal cut through the ventricular cone (Fig. 24). The current inconsistencies in nomenclature of the echocardiographic ventricular segments, therefore, can be made anatomically accurate simply by describing septal and lateral quadrants in addition to those which, on direct observation, are self-evidently seen to be located superiorly and inferiorly (Fig. 25).

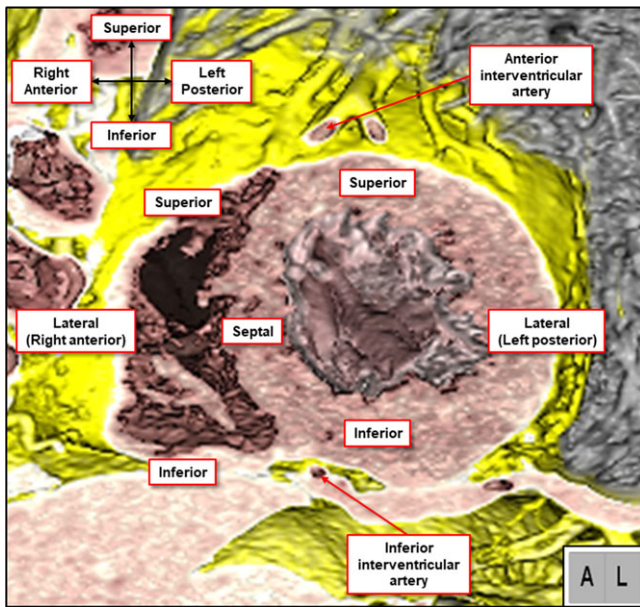


Fig. 25. The virtual dissection is made to show a short axis cut across the ventricular cone as viewed from the left anterior oblique 45° direction. As shown, the four quadrants of the cone can accurately be described as being superior, inferior, septal, and lateral. Note we have labeled the interventricular artery occupying the superior inferior interventricular groove as being anterior, since it does run anteriorly as it extends to the ventricular apex, and its blockage does produce antero-septal myocardial infarction. The artery within the inferior interventricular groove, however, is correctly identified as being inferior, with its blockage producing inferior myocardial infarction. [Color figure can be viewed at wileyonlinelibrary.com]

CONCLUSIONS

Careful virtual dissection of three-dimensional datasets obtained from living patients now permits demonstration of all the necessary details of cardiac anatomy, paralleling the information that can be revealed by true dissection of cadaveric or autopsied hearts. Since the datasets are obtained with the individuals in the anatomical position, however, the components are readily described following the basic rules of human anatomy, in other words, in attitudinally appropriate fashion. These subtle features of the cardiac structural anatomy, furthermore, are demonstrated without distortion of their spatial relationships within the thorax. There is now no reason why images such as we have produced should not be used to illustrate cardiac anatomy in all standard textbooks as used for the teaching of medical students and clinical trainees. This, in turn, should serve to emphasize the need also for anatomy to be taught using attitudinally appropriate nomenclature. When combined with the accumulated basic anatomical information, such approaches will surely bridge the gap currently existing between the dissection room and the clinical setting, helping

to persuade clinicians also to adopt the attitudinal nomenclature.

ACKNOWLEDGMENTS

The authors thank Professor Ken-ichi Hirata, from the Division of Cardiovascular Medicine, Department of Internal Medicine, Kobe University Graduate School of Medicine, for providing an opportunity for continuous investigation of living cardiac anatomy. We also thank all of our colleagues in the cardiac imaging group (Shinsuke Shimoyama, Yu Izawa, Takayoshi Toba, Daisuke Tsuda, Hiroyuki Toh, Masataka Suzuki, Yu Takahashi, Takuro Nishio, Tomoki Maebayashi, Wakiko Tani, Kiyosumi Kagawa, and Noriyuki Negi) of Kobe University Graduate School of Medicine, without whose help it would have been impossible to produce the virtual dissections as shown in our review.

CONFLICTS OF INTEREST

The authors have no conflicts of interest.

REFERENCES

- Anderson RH, Ho SY, Becker AE. 2000. Anatomy of the human atrio-ventricular junctions revisited. *Anat Rec* 260:81–91.
- Anderson RH. 2000. Clinical anatomy of the aortic root. *Heart* 84: 670–673.
- Anderson RH. 2001. How do we determine atrial arrangement? *Cardiol Young* 11:482–483.
- Anderson RH, Webb S, Brown NA, Lamers W, Moorman A. 2003a. Development of the heart: (3) formation of the ventricular outflow tracts, arterial valves, and intrapericardial arterial trunks. *Heart* 89:1110–1118.
- Anderson RH, Webb S, Brown NA, Lamers W, Moorman A. 2003b. Development of the heart: (2) Septation of the atriums and ventricles. *Heart* 89:949–958.
- Anderson RH, Razavi R, Taylor AM. 2004. Cardiac anatomy revisited. *J Anat* 205:159–177.
- Anderson RH, Cook AC. 2007. The structure and components of the atrial chambers. *Europace* 9:vi3–vi9.
- Anderson RH, Loukas M. 2009. The importance of attitudinally appropriate description of cardiac anatomy. *Clin Anat* 22:47–51.
- Anderson RH, Spicer DE, Hlavacek AJ, Hill A, Loukas M. 2013. Describing the cardiac components—attitudinally appropriate nomenclature. *J Cardiovasc Transl Res* 6:118–123.
- Anderson RH, Mohun TJ, Spicer DE, Bamforth SD, Brown NA, Chaudhry B, Henderson DJ. 2014. Myths and realities relating to development of the arterial valves. *J Cardiovasc Dev Dis* 1: 177–200.
- Anderson RH. 2015. Re-setting the gold standard. *J Cardiovasc Electrophysiol* 26:713–714.
- Anderson RH, Mori S, Spicer DE, Brown NA, Mohun TJ. 2016. Development and morphology of the ventricular outflow tracts. *World J Pediatr Congenit Heart Surg* 7:561–577.
- Anderson RH, Mori S. 2016. How can we best describe the cardiac components? *J Cardiovasc Electrophysiol* 27:972–975.
- Anderson RH, Bolender D, Mori S, Tretter JT. 2018a. Virtual reality perhaps, but is this real cardiac anatomy? *Clin Anat*. <https://doi.org/10.1002/ca.23306>. [Epub ahead of print].
- Anderson RH, Mohun TJ, Sánchez-Quintana D, Mori S, Spicer DE, Cheung JW, Lerman BB. 2018b. The anatomic substrates for outflow tract arrhythmias. *Heart Rhythm*. <https://doi.org/10.1016/j.hrthm.2018.08.014>. [Epub ahead of print].

- Anderson RH, Mori S, Spicer DE, Cheung JW, Lerman BB. 2018c. Living anatomy of the pulmonary root. *J Cardiovasc Electrophysiol* 29:1238–1240.
- Becker AE, Anderson RH. 1982. Atrioventricular septal defects: What's in a name? *J Thorac Cardiovasc Surg* 83:461–469.
- Cerqueira MD, Weissman NJ, Dilsizian V, Jacobs AK, Kaul S, Laskey WK, Pennell DJ, Rumberger JA, Ryan T, Verani MS, American Heart Association Writing Group on Myocardial Segmentation and Registration for Cardiac Imaging. 2002. Standardized myocardial segmentation and nomenclature for tomographic imaging of the heart: A statement for healthcare professionals from the cardiac imaging Committee of the Council on clinical cardiology of the American Heart Association (review). *Circulation* 105:539–542.
- Cosío FG, Anderson RH, Kuck KH, Becker A, Borggrefe M, Campbell RW, Gaita F, Guiraudon GM, Haissaguerre M, Ruflanchas JJ, Thiéne G, Wellens HJ, Langberg J, Benditt DG, Bharati S, Klein G, Marchlinski F, Saksena S. 1999. Living anatomy of the atrioventricular junctions. A guide to electrophysiologic mapping. A Consensus Statement from the Cardiac Nomenclature Study Group, Working Group of Arrhythmias, European Society of Cardiology, and the task force on cardiac nomenclature from NASPE. *Circulation* 100:e31–e37.
- Crucean A, Brawn WJ, Spicer DE, Franklin RC, Anderson RH. 2014. Holes and channels between the ventricles revisited. *Cardiol Young* 23:1–12.
- Dean JW, Ho SY, Rowland E, Mann J, Anderson RH. 1994. Clinical anatomy of the atrioventricular junctions. *J Am Coll Cardiol* 24:1725–1731.
- Farré J, Anderson RH, Cabrera JA, Sánchez-Quintana D, Rubio JM, Benezet-Mazuecos J, Del Castillo S, Maciá E. 2010. Cardiac anatomy for the interventional arrhythmologist: I. Terminology and fluoroscopic projections. *Pacing Clin Electrophysiol* 33:497–507.
- Holda MK, Stefura T, Koziej M, Skomarowska O, Jasińska KA, Sałabun W, Klimek-Piotrowska W. 2019. Alarming decline in recognition of anatomical structures amongst medical students and physicians. *Ann Anat* 221:48–56.
- Jacobs JP, Anderson RH, Weinberg PM, Walters HL 3rd, Tchervenkov CI, Del Duca D, Franklin RC, Aiello VD, Béland MJ, Colan SD, Gaynor JW, Krogmann ON, Kurosawa H, Maruszewski B, Stellin G, Elliott MJ. 2007. The nomenclature, definition and classification of cardiac structures in the setting of heterotaxy. *Cardiol Young* 17:1–28.
- Jensen B, Spicer DE, Sheppard MN, Anderson RH. 2017. Development of the atrial septum in relation to postnatal anatomy and interatrial communications. *Heart* 103:456–462.
- Lamers WH, Moorman AF. 2002. Cardiac septation: A late contribution of the embryonic primary myocardium to heart morphogenesis. *Circ Res* 91:93–103.
- Lang RM, Badano LP, Mor-Avi V, Afilalo J, Armstrong A, Ernande L, Flachskampf FA, Foster E, Goldstein SA, Kuznetsova T, Lancellotti P, Muraru D, Picard MH, Rietzschel ER, Rudski L, Spencer KT, Tsang W, Voigt JU. 2015. Recommendations for cardiac chamber quantification by echocardiography in adults: An update from the American Society of Echocardiography and the European Association of Cardiovascular Imaging. *J Am Soc Echocardiogr* 28:1–39.
- Loomba RS, Hlavacek AM, Spicer DE, Anderson RH. 2015. Isomerism or heterotaxy: Which term leads to better understanding? *Cardiol Young* 25:1037–1043.
- Loukas M, Aly I, Tubbs RS, Anderson RH. 2016. The naming game: A discrepancy among the medical community. *Clin Anat* 29:285–289.
- Maresky HS, Oikonomou A, Ali I, Ditkowsky N, Pakkal M, Ballyk B. 2018. Virtual reality and cardiac anatomy: Exploring immersive three-dimensional cardiac imaging, a pilot study in undergraduate medical anatomy education. *Clin Anat*. <https://doi.org/10.1002/ca.23292>. [Epub ahead of print].
- Merrick AF, Yacoub MH, Ho SY, Anderson RH. 2000. Anatomy of the muscular subpulmonary infundibulum with regard to the Ross procedure. *Ann Thorac Surg* 69:556–561.
- Mori S, Nishii T, Takaya T, Kashio K, Kasamatsu A, Takamine S, Ito T, Fujiwara S, Kono AK, Hirata K. 2015a. Clinical structural anatomy of the inferior pyramidal space reconstructed from the living heart: Three-dimensional visualization using multidetector-row computed tomography. *Clin Anat* 28:878–887.
- Mori S, Fukuzawa K, Takaya T, Takamine S, Ito T, Fujiwara S, Nishii T, Kono AK, Yoshida A, Hirata K. 2015b. Clinical structural anatomy of the inferior pyramidal space reconstructed within the cardiac contour using multidetector-row computed tomography. *J Cardiovasc Electrophysiol* 26:705–712.
- Mori S, Fukuzawa K, Takaya T, Takamine S, Ito T, Kinugasa M, Shigeru M, Fujiwara S, Nishii T, Kono AK, Yoshida A, Hirata K. 2015c. Optimal angulations for obtaining an en face view of each coronary aortic sinus and the interventricular septum: Correlative anatomy around the left ventricular outflow tract. *Clin Anat* 28:494–505.
- Mori S, Spicer DE, Anderson RH. 2016a. Revisiting the anatomy of the living heart. *Circ J* 80:24–33.
- Mori S, Fukuzawa K, Takaya T, Takamine S, Ito T, Fujiwara S, Nishii T, Kono AK, Yoshida A, Hirata K. 2016b. Clinical cardiac structural anatomy reconstructed within the cardiac contour using multidetector-row computed tomography: The arrangement and location of the cardiac valves. *Clin Anat* 29:364–370.
- Mori S, Fukuzawa K, Takaya T, Takamine S, Ito T, Fujiwara S, Nishii T, Kono AK, Yoshida A, Hirata K. 2016c. Clinical cardiac structural anatomy reconstructed within the cardiac contour using multidetector-row computed tomography: Atrial septum and ventricular septum. *Clin Anat* 29:342–352.
- Mori S, Fukuzawa K, Takaya T, Takamine S, Ito T, Fujiwara S, Nishii T, Kono AK, Yoshida A, Hirata K. 2016d. Clinical cardiac structural anatomy reconstructed within the cardiac contour using multidetector-row computed tomography: Left ventricular outflow tract. *Clin Anat* 29:353–363.
- Mori S, Anderson RH, Tahara N, Izawa Y, Toba T, Fujiwara S, Shimoyama S, Watanabe Y, Nishii T, Kono AK, Hirata KI. 2017a. Diversity and determinants of the three-dimensional anatomical Axis of the heart as revealed using multidetector-row computed tomography. *Anat Rec (Hoboken)* 300:1083–1092.
- Mori S, Anderson RH, Takaya T, Toba T, Ito T, Fujiwara S, Watanabe Y, Nishii T, Kono AK, Hirata KI. 2017b. The association between wedging of the aorta and cardiac structural anatomy as revealed using multidetector-row computed tomography. *J Anat* 231:110–120.
- Mori S, Anderson RH, Nishii T, Matsumoto K, Loomba RS. 2017c. Isomerism in the setting of the so-called "heterotaxy": The usefulness of computed tomographic analysis. *Ann Pediatr Cardiol* 10:175–186.
- Mori S, Anderson RH, Tahara N, Izawa Y, Toba T, Fujiwara S, Shimoyama S, Watanabe Y, Nishii T, Kono AK, Takahashi S, Hirata KI. 2017d. The differences between bisecting and off-center cuts of the aortic root: The three-dimensional anatomy of the aortic root reconstructed from the living heart. *Echocardiography* 34:453–461.
- Mori S, Nishii T, Tretter JT, Spicer DE, Hirata KI, Anderson RH. 2018a. Demonstration of living anatomy clarifies the morphology of interatrial communications. *Heart* 104:2003–2009.
- Mori S, Tretter JT, Toba T, Izawa Y, Tahara N, Nishii T, Shimoyama S, Tanaka H, Shinke T, Hirata KI, Spicer DE, Saremi F, Anderson RH. 2018b. Relationship between the membranous septum and the virtual basal ring of the aortic root in candidates for transcatheter implantation of the aortic valve. *Clin Anat* 31:525–534.
- Sievers HH, Hemmer W, Beyersdorf F, Moritz A, Moosdorf R, Lichtenberg A, Misfeld M, Charitos EI, Working Group for Aortic Valve Surgery of German Society of Thoracic and Cardiovascular Surgery. 2012. The everyday used nomenclature of the aortic root components: The tower of Babel? *Eur J Cardiothorac Surg* 41:478–482.
- Spicer DE, Bridgeman JM, Brown NA, Mohun TJ, Anderson RH. 2014. The anatomy and development of the cardiac valves. *Cardiol Young* 24:1008–1022.

- Stanford W, Erkonen WE, Cassell MD, Moran BD, Easley G, Carris RL, Albanese MA. 1994. Evaluation of a computer-based program for teaching cardiac anatomy. *Invest Radiol* 29:248–252.
- Sutton JP 3rd, Ho SY, Anderson RH. 1995. The forgotten interleaflet triangles: A review of the surgical anatomy of the aortic valve. *Ann Thorac Surg* 59:419–427.
- Tretter JT, Spicer DE, Mori S, Chikkabyrappa S, Redington AN, Anderson RH. 2016. The significance of the interleaflet triangles in determining the morphology of congenitally abnormal aortic valves: implications for noninvasive imaging and surgical management. *J Am Soc Echocardiogr* 29:1131–1143.
- Tretter JT, Mori S, Saremi F, Chikkabyrappa S, Thomas K, Bu F, Loomba RS, Alsaied T, Spicer DE, Anderson RH. 2018. Variations in rotation of the aortic root and membranous septum with implications for transcatheter valve implantation. *Heart* 104: 999–1005.
- Uemura H, Ho SY, Devine WA, Kilpatrick LL, Anderson RH. 1995. Atrial appendages and venoatrial connections in hearts from patients with visceral heterotaxy. *Ann Thorac Surg* 60:561–569.
- Webb S, Qayyum SR, Anderson RH, Lamers WH, Richardson MK. 2003. Septation and separation within the outflow tract of the developing heart. *J Anat* 202:327–342.
- Willens HJ, Kessler KM. 2000. Transesophageal echocardiography in the diagnosis of diseases of the thoracic aorta: Part II—atherosclerotic and traumatic diseases of the aorta. *Chest* 117: 233–243.